CONTINUOUS DRAWING STUDIES OF FOAM FIBRILLATED YARN

A THESIS

Presented to

The Faculty of the Division of Graduate Studies

by

Jack Douglas Childs

In Partial Fulfillment

of the Requirements for the Degree

Masters of Science

in the School of Chemical Engineering

Georgia Institute of Technology

November 1978

CONTINUOUS DRAWING STUDIES

OF

FOAM FIBRILLATED YARN

Approved:

John D. Muzzy, Chairman

W. D. Freeston

Gary W. Poehlein

Date approved by Chairman Nov. 30, 1978

ACKNOWLEDGMENTS

The author wishes to thank his thesis advisor, Dr. John D. Muzzy, for his concern and guidance throughout the course of this project.

The fellowship sponsored by Gulf Oil Corporation is greatly appreciated. The Chemical Engineering Department is thanked for providing a Graduate Teaching Assistantship for the 1978 Fall Quarter.

The author is indebted for the efficient assistance of several staff members associated with this project, especially Anil Enuga and Guillermo Hoyos who worked out most of the bugs and compiled much of the data for this work. The author thanks Ed Cohne for his time and his willingness to share his expertise with the X-ray machinery and the electron microscope.

Appreciation is extended to Dr. W. D. Freeston and Dr. G. W. Poehlein for having served on the reading committee in the midst of their busy schedules.

TABLE OF CONTENTS

TABLE OF CONTENTS

LIST OF ILLUSTRATIONS

LIST OF ILLUSTRATIONS

SUMMARY

A polypropylene yarn can be extruded by a novel foam fibrillation process that has commercial potential. A polymer melt containing a blowing agent was extruded through a circular annulus and biaxially stretched over a circular mandrel resulting in a fibrous web. As extruded, the yarn has the disadvantages of high linear density and low strength, therefore drawing and twisting is needed to improve the properties.

The conditions for continuous drawing were investigated in this study to determine their effects on the structure and properties of the yarn. The continuous drawing system consisted of a hot air oven situated between calibrated rollers that could be manipulated to produce variable draw ratios and oven residence times. The structural effects of drawing and twisting were studied using: (1) X-ray diffraction to measure the crystallinity and the crystal orientation, (2) optical birefringence to measure the relative change in molecular orientation, and (3) optical and electron microscopy for visual inspection of the yarn cross sections and longitudinal structure. The yarn structure was correlated with the process parameters and elongation and tenacity.

Continuous drawing of the yarn can produce yarns with tenacities of commercial value (greater than 2 g/denier). It is found that drawing causes the tenacity to increase while the elongation asymptotically approaches 15 to 25% at break for a draw ratio of four. Twist is needed to provide the undrawn yarn enough strength to successfully draw it in

the continuous drawing system.

Investigation of the variables involved in drawing shows that the actual draw ratio obtained is most important in determining the tenacity of the yarn. Twist produced an optimum tenacity at 5 TPI for a yarn drawn four times. The temperature and rate of elongation of the yarn in the drawing oven did not have an effect on the tenacity or elongation at break over the range studied.

Structural study indicated a constant increase in molecular orientation as the actual draw ratio increases. The ribbon shaped filaments decrease in size with increasing draw ratio while the number of filaments increases. The size distribution of filaments becomes sharper as the draw ratio is increased.

The molecular orientation morphology due to drawing is similar to that of monofilaments made of polypropylene. The effect of twist on the foam fibrillated yarn is similar to commercial staple fiber yarn.

CHAPTER I

INTRODUCTION

1.1 Statement of the Problem

With the advent of synthetic fiber capabilities, the textile industry has looked to research for processing techniques to circumvent the prevailing high operating costs and multiple processing steps which characterize yarn manufacturing [1-6]. The traditionally high operating leverage of the fiber industry has limited processes to large scale production operations [1,4,5]. Presently, the workhorse of the synthetic fiber processes is melt spinning which is expensive to operate. In this process, a polymer is extruded under high pressure through a very small die. The fine continuous filaments emerging from the die can be used for continuous filament yarns or they can be chopped and used for the feed material in the production of staple yarns. Thermoplastic filaments are drawn, crimped, heat set, and cut before the conventional drawing and spinning of the staple yarn process. The use of continuous filament yarns circumvents the need for so many processing steps but in order to achieve a desirable bulk, comfort, and dimensional stability, texturizing processes must be introduced. The texturizing, achieved by edge crimping, gear crimping, air jet, and false twisting processes, causes permanent waviness (crimp), coils and wrinkles [7]. The development of a simplified process route which results in a yarn like staple fiber yarn has not been attained but the need for such a process is increasing.

Research has developed a range of alternate yarn formation techniques. One direction of these processes is aimed at exploiting the natural tendency for thermoplastic polymer films to break down into fine fibrous strips upon drawing. The strips can be separated at their boundaries, fibrillated, to form a network of filaments from the sheet by using various mechanical methods. A recent evolution of these processes incorporates the three-dimensional network formed from extrusion of a polymer foam with the polymer's inherent property of fibrillation to form a novel yarn [7-11]. The foam emerging from an annular slit die is cooled and biaxially stretched over a conical mandrel which causes the polymer to fibrillate into filaments. The continuous drawing of the novel yarn would complete the processing necessary to attain a strong yarn suitable for commercial use provided that drawing conditions can be achieved that allow sufficient molecular orientation, the structural feature most important in increasing tenacity [12].

The network yarn formed has properties unique in comparison to traditional yarns. The network yarn exhibits the highly desired quality of bulk attained mainly by staple yarns and it has the possibility of stronger tenacities. The yarn can be used without twist just like continuous filament yarns but an untwisted network has not yet been processed to achieve comparable tenacities. A widely used yarn since the 60's, mechanically fibrillated film yarns are a two-dimensional analog of the three-dimensional network yarns, yet they have a coarser texture, so their applications have been limited [1].

Polypropylene has been used in many new film fibrillation processes, because of its superior processing properties and the development

of markets for film fibrillated yarn. Foam fibrillation followed with biaxial stretching demands a polymer with high melt strength (tensile viscosity) and polypropylene accommodates that demand [5,8]. Foam fibrillation is an intermediate processing technique between the mechanically fibrillated film to fiber process and flash spinning [8,9]. In flash spinning, a polymer solution and a dispersed vapor are extruded with the vapor expanding and separating as the extrudate emerges from the die. The flashing phase prevents coalescence of the fibrils, thus forming a network yarn [9].

Foam fibrillation with biaxial stretching provides the potential of forming finer structures than mechanically fibrillated films, without involvement of a solvent recovery system as in flash spinning. Stretching the foam ruptures the bubbles in the emerging extrudate resulting in a three-dimensional network of filaments. The addition of a conical mandrel stretches the foam biaxially, leading to more complete and uniform fibrillation of the yarn. In this process, the fibrillation takes place as the cooled web stretches over the mandrel of increasing diameter, therefore causing the web to increase its circumference by splitting at the fibril boundaries.

This thesis studies the effects of drawing conditions on the properties of the fibrillated foam yarn. Evaluation of the range of properties available through drawing provides quantitative information to assess the value of the yarn to the market. A drawing unit which could produce yarns at a speed that would allow simultaneous extrusion and drawing in line as a continuous process is desired.

1.2 Evolution of the Process

In the 1930's, H. Jacque of I. G. Farbenindustrie found that poly (vinylchloride) produced a microfibrous morphology when stretched. The polymer sheet, when drawn 45 times, was oriented enough to recognize individual fibrils within the film. The high draw ratio and the lack of commercially available polymers that worked, made the process unfeasible [1,5].

Scattered attempts were made to use the idea, but no real progress was made until Natta developed stereospecific polymerization catalysts which allowed the production of highly crystalline polyolefins [1,5,10]. These polymer films fibrillated at much lower draw ratios and they had considerably higher tenacities [1].

Polypropylene was found to fibrillate easily and it had a melting point just high enough to be used as a fiber in the textile industry [16]. The film to fiber route grew, using polypropylene as a major material, and split fibers became available as a coarse textured, yet cheaply produced yarn.

The 1960's brought with them a rise in the price of natural fibers used for ropes and twine, such as hemp and sisal [1,5]. The split polypropylene fibers became competitive with the natural fibers on a strength to cost scale [1,5]. Polypropylene's hydrophobic character also made it attractive for marine applications [1,15].

Slit films (films drawn and cut in narrow strips) were introduced as an alternative to the split fibrillation method. Both slit and split films found success in the coarse fiber market but their limiting coarse texture prevented their move into other markets, such as garments [1].

Fibrillation techniques were approached by many methods; the best methods produced filaments as fine as five denier [1,5]. Film fibrillation was commonly done in the solid phase and the natural fibrillation was enhanced by a mechanical stimulus such as a pinwheel fibrillator [2-5,13,14]. It was found that the blending of incompatible or even semicompatible polymers produced a finer fibrillation on drawing. Likewise, embossing the film accentuated the natural fibrillation mechanism [6]. The possibilities of producing a structure fine enough for apparel fabric were growing.

The concept of a three-dimensional network structure formed from a foam seemed equitable as a solution to the two-dimensional network's coarse texture. The cell walls of an erupted foam bubble had the potential of producing a fine structure if the bubbles could be made of uniform size. Flash spinning offered the uniformity of bubbles by using a foaming agent that was soluble in the polymer [9]. The bubbles were well dispersed at the expense of a solvent that demanded recovery. The use of nitrogen and carbon dioxide are currently being suggested as solvents for flash spinning which do not need to be recovered [9].

Foam fibrillation has several available routes to the formation of a fiber. This study involves a foam fibrillated process developed by Schirmer [8] which biaxially stretches the foam as it cools, thereby separating fibrils as the diameter of the foam web expands to conform to the mandrel. The further processing of the yarn by drawing is considered necessary to increase the strength and to make the multiple diameter filaments more uniform. The aim of the project is to ultimately produce a commercially desirable yarn in a continuous process directly from the

extruder, with the minimum necessary process steps.

1.3 Fiber Drawing

Undrawn foam fibrillated yarns exhibit low tenacity and high elongation when first formed. This study investigates the drawing of the network yarn by using heat and tension to induce orientation of the molecules with the fiber axis. Used extensively for continuous filament yarns, drawing causes irreversible elongation along the fiber axis, which improves the tenacity and modulus [12,15,16]. The elongation causes alignment of the molecules with the fiber axis, which gives strength in the axial direction. In addition to improving the tenacity, the drawing is also aimed at reducing the size distribution of filaments in the yarn by separating the large filaments by further fibrillation [12,16].

The degree of molecular orientation is dependent on the drawing conditions, the composition, and the history of the feed material. Two important parameters in drawing are temperature and the rate of elongation of the fiber. Since test runs are at temperatures sufficiently higher than the temperatures at which polypropylene exhibits necking or non-uniform type deformation, uniform elongation occurs. As temperature is increased, the molecular mobility increases, therefore the maximum draw ratio increases. As the material approaches the melting point, it weakens and the ultimate deformation is reached more easily. These tendencies cause a maximum drawing temperature to be observed in many systems [12].

The rate of deformation is also important as a drawing parameter because polypropylene is viscoelastic in nature. An increase in

deformation rate at constant temperature causes the stress-strain curve to react just as it does with a decrease in temperature. The effect of deformation is not that simple, however; much of the energy used to deform the polymer is dissipated as heat. If the deformation is fast enough, the effect of a temperature rise due to deformation can override the viscoelastic effect. This effect is most prevalent in non-uniform necking deformation fortunately [12].

The amount of orientation induced by elongation changes the properties of the polymer, therefore the polymer's response to temperature and deformation rate changes with its molecular orientation. Crystallinity changes affect the fiber's response to the drawing conditions. An increase in crystallinity modifies the stress-strain relation toward non-uniform deformation (necking type) and leads to higher yield stresses. As processing temperatures approach the melting temperature, the crystallization or destruction of crystals happens more often, depending on the polymer and its crystallization kinetics [12].

Drawing tension is an empirical characteristic of technical drawing which is important when determining draw conditions. This parameter is useful in visualizing the change in elongation rate along the length of the hot air drawing box. Not only does the molecular orientation change as the fiber length goes through the drawing process, but the temperature, deformation rate, and sometimes the crystallinity of the fiber at any location affect the elongation at the other locations in the box. Each parameter's response depends on the stress in the line [12].

The network yarn has several structural levels of interest. The

drawing will have an effect on each level but it can be confusing if the nomenclature is not defined. The network yarn's overall structure is referred to as the superstructure, while the interconnected members making up that web are described as the filaments and the bundle of fibrillar structures (not visible with the naked eye) that make up the filaments are called fibrils.

1.4 Previous Studies

Hand drawing of foam fibrillated yarn has been investigated by Park [17]. He found that tenacity was increased significantly by drawing and twisting with a maximum at a drawing temperature of 130°C. A maximum tenacity was also observed for a twist of 5TPI and elongation at break decreased as the draw ratio increased. It was indicated from microscopic observation that the filament diameter became finer as the draw ratio increased, yielding a sharper filament diameter distribution [17].

Park's study of hand drawing is compared to the continuous process used in this study. A comparison to traditional textile yarns is also used to evaluate the properties of the continuously drawn foam fibrillated yarn.

CHAPTER II

EQUIPMENT AND MATERIALS

2.1 Process Equipment

A screw extruder (Rheomex® 254, Haake, Inc.) with a 3/4" barrel diameter and 25:1 length to diameter ratio was used to extrude the foam (see Figure 1). Five temperature control zones maintained a previously determined temperature profile along the barrel and die [11]. The annular die had an outside diameter of 1" with a .08" annular slit.

The stretching mandrel was attached to the die by means of a rod screwed into the center of the die. The mandrel diameter was 2-1/2" at the base which was positioned 3" below the die.

Continuous drawing of the yarn was achieved using a 7' long wooden box which was 4" by 4" in cross section (see Figure 2). The box was positioned between calibrated feed and take-up rollers. Hot air was supplied at specific temperatures by an electrically heated air dryer (Desikator®, Polymer Machinery Corporation). The air was recycled back to the dryer. The desiccant bed in the dryer was bypassed, hence, no moisture was removed from the air.

Twisting was accomplished by rotations of a bobbin of yarn about a vertical axis and continuously collecting the yarn from the bobbin at a calibrated rate (see Figure 3).

2.2 Testing Equipment

An Instron Engineering Corporation Tensile Tester (Model TTC) was

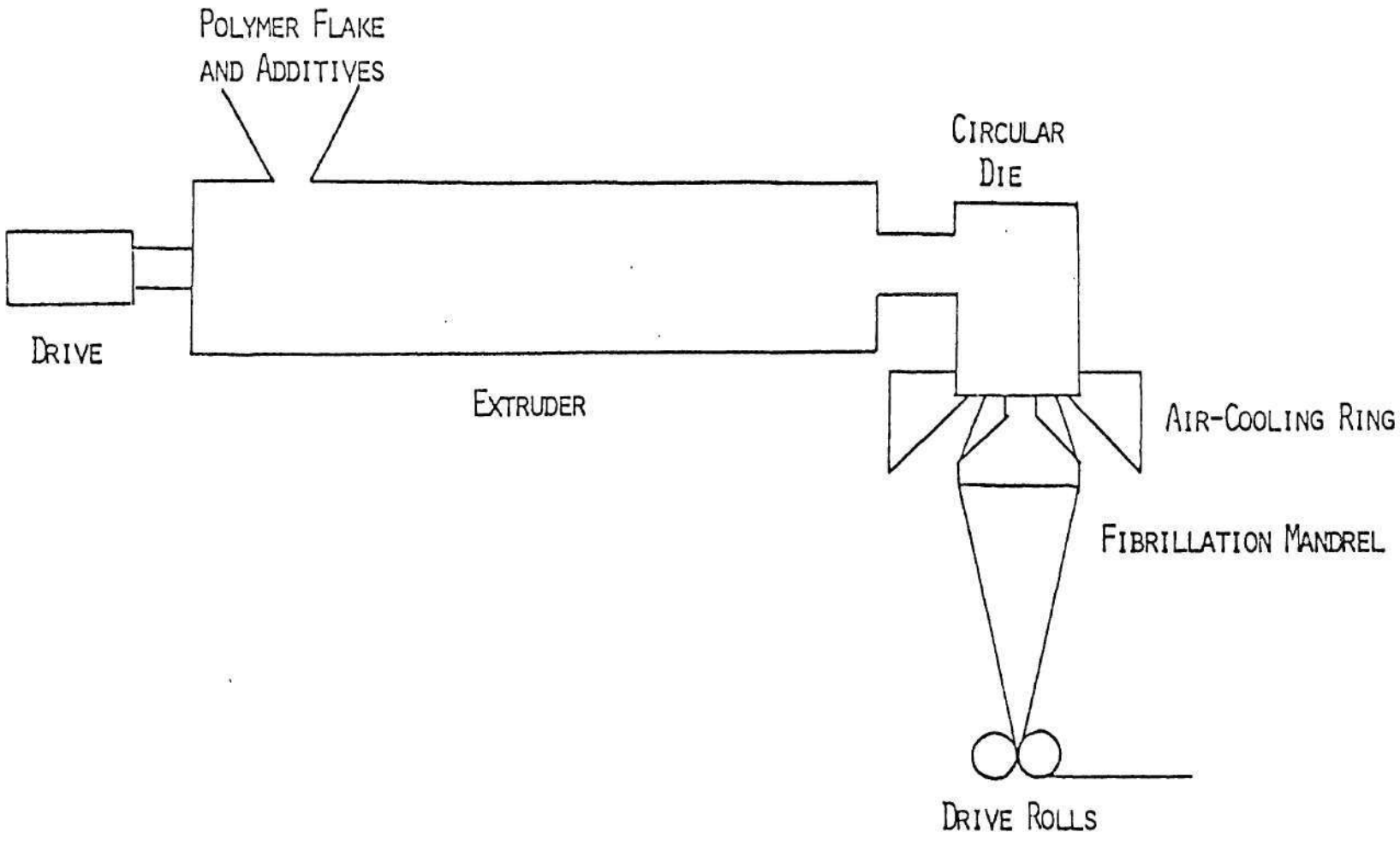

Figure 1. Extruder Unit with Mandrel

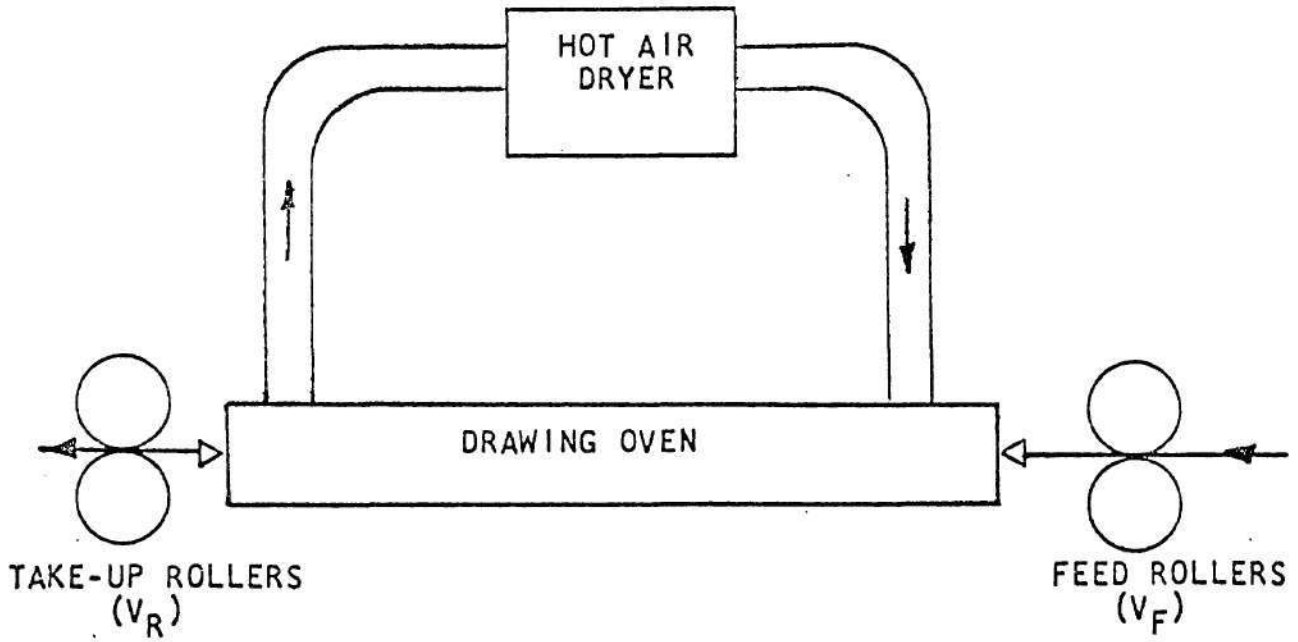

Figure 2. Continuous Drawing System

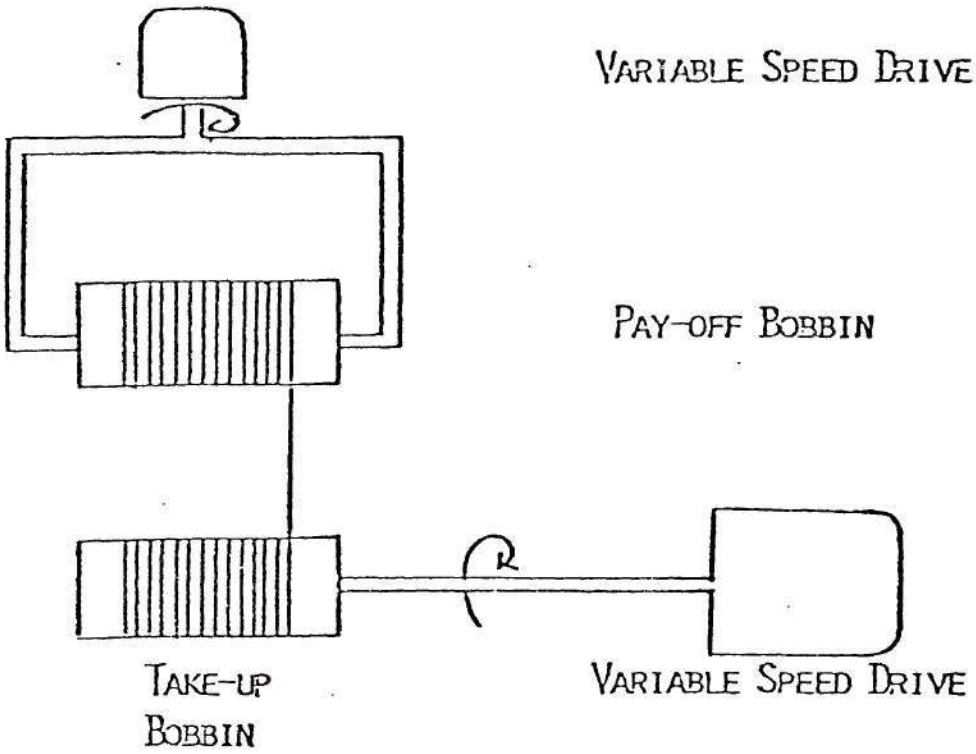

Figure 3. Twisting Apparatus

used to measure the tenacity and elongation at break of the yarn samples.

A Zeiss polarizing light microscope was used to determine the birefringence of the drawn fibers. Oils with a range of calibrated refractive indices from 1.4 to 1.7 in .004 increments were used in conjunction with the light microscope. These oils were obtained from R. P. Cargille Laboratories.

A Jeol JEM-100C Electron Microscope was used to inspect the quality of the junctions at varying magnifications using the scanning electron microscope ability of the machine. Gold-palladium alloy from Scan-Atlanta was used to coat the sample fibers.

A Siemens Krystalloflex 4 was used in the determination of the intensity of diffracted peaks for orientation studies. The crystallinity of the fibers was measured using a General Electric Diffractometer (XRD-4).

Cross sections of the fibers were viewed and photographed using a Vickers Fifty-five Microscope from Cooke Company.

2.3 Materials

Isotactic polypropylene (Profax 6323) was obtained in flake form from Hercules Chemical Corporation. The melt index, taken from the manufacturer's literature was 12.0 g/min. at 230°C. Polypropylene was selected because of its advantages as a fiber and its easy processing character [2-5,14].

The blowing agent was Kempore® 200MC, an azodicarbonamide which was obtained from Stepan Chemical Company. This blowing agent was best suited for the temperatures used in extrusion [19,20,27].

CHAPTER III

EXPERIMENTAL PROCEDURES

3.1 Processing

Extrusion

The extrusion parameters were held constant so as to produce a consistent parent yarn and maintain an emphasis on the drawing process. The extrusion conditions had been studied in a previous experiment; therefore, a set of conditions were used that allowed continuous extrusion but produced a yarn that was not filmy [11]. The polypropylene was in flake form; therefore, it could be thoroughly mixed by hand with the azodicarbonamide on a weight basis using 1% blowing agent. Blending did not seem to be a problem judging from the uniformity of the foam web produced. The feed material was fed into the extruder at the hopper. The five temperature control zones maintained a temperature profile starting at the feed of 200, 230, 240, 240, and 240°C. The extruder's screw speed was 20 RPM. The extrudate emerged from the die and was quenched with an annular flow of air expanding from 10 psig. The web was biaxially stretched over the mandrel and wound up at 65 feet per minute.

Drawing and Twisting

The undrawn yarn was initially twisted to induce two turns per inch (2TPI) before drawing. The hot air box was placed between two rollers which were calibrated for varying speeds. The temperature was set on the hot air supply and the feed velocity was calibrated at the

beginning of the box. The draw ratio was determined by calibrating the take-up roller with a velocity equal to the feed velocity times the draw ratio. Sequential twisting and drawing was done in several test runs.

3.2 Testing

Tensile Strength and Elongation at Break

The breaking strength and elongation at break were measured using a tensile tester at 70°F with a 5 inch gauge length, 100% per minute extrusion rate, and a 5 inch per minute chart speed. The linear density of the yarn was measured in denier (the gram weight of 9000 meters of yarn). The breaking strength was recorded as grams per denier and referred to as tenacity.

Actual Draw Ratio

The actual draw ratio was determined as the ratio of the denier of the undrawn yarn to the denier of the drawn yarn. This method assumes affine deformation.

Birefringence

The yarn sample was cut into small filaments using a razor, being careful not to stretch the filaments. The yarn was then immersed in a liquid with approximately the same index of refraction as the yarn, and then a bright line (Becke line) between the boundary of the filament and the liquid was observed. Since the Becke line moves toward the medium of higher refractive index as the objective lens is raised from the sample, the refractive index of the filament can be resolved by trial and error using different oils. Using polarized light allows separate determination of the index of refraction in the axial and the transverse direction. The birefringence is a measure of the difference between the

axial and transverse index of refraction of the filament [20].

Measurement of the Filament Cross Section

The yarn samples were embedded in Sear's epoxy resin which was made opaque by adding ultrafine carbon black. The samples were sanded and polished, ending with a 10 micron polish. The samples were then photographed using the Vicker's Fifty-five microscope. Since the magnification was known, the enlarged photographs could be directly measured and the sizes calculated.

X-ray Determination of Crystallinity and Orientation

The literature has presented a technique to measure the crystallinity by graphical integration of the diffraction pattern for polypropylene [21]. The technique is empirical in nature. Assumptions involve an equal electron density for each unit mass of amorphous and crystalline phases and an intensity linearly dependent on the percentages of crystalline and amorphous phases [23] (see Appendix B).

The orientation of the crystalline phase of the polymer can be determined from integration of diffraction intensities of specific planes in the crystal with respect to angular position from the fiber axis [23,24]. The orientation of polypropylene has been studied previously for continuous filament yarns and X-ray procedures have been devised [24,26] (see Appendix A).

CHAPTER IV

RESULTS AND DISCUSSION

4.1 Introduction

Hand drawing of a foam fibrillated network yarn has been investigated by Park [17]. Temperature, twist, and draw ratio were shown to affect the tenacity of the hand drawn yarn. The continuous drawing of the foam fibrillated yarn is investigated by varying the rate of elongation in addition to the hand drawn variables. The rate of elongation in this continuous drawing system is dependent on the feed velocity to the drawing oven and the amount of elongation imposed on the yarn while in the oven.

Park determined that twisting and drawing improved the tenacity in the hand drawing process. In the continuous drawing process, a certain minimum twist was necessary to give the undrawn yarn enough strength that it could be drawn without breakage; therefore, all undrawn yarns were initially twisted two turns per inch (TPI) prior to any drawing. This twisting provided a helical angle of twist of 43 degrees [25].

4.2 Actual Draw Ratio

The effect of actual draw ratio on tenacity and elongation at break holding the feed velocity, temperature, and twist constant is illustrated in Figure 4. The tenacity increases with increasing actual draw ratio as the elongation at break asymptotically decreases. These trends are in good agreement with Park's findings for hand drawing [17] (see Figure 5).

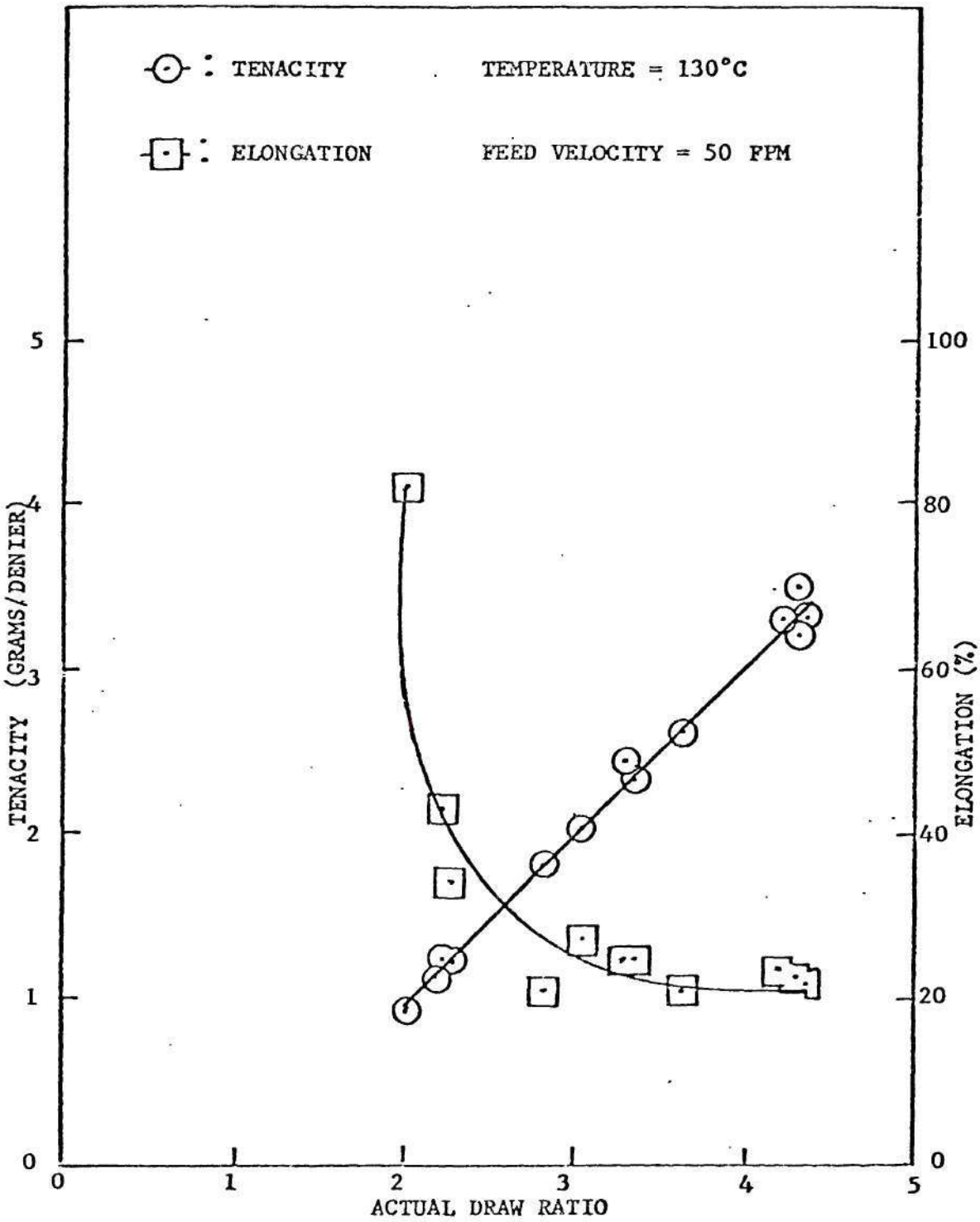

Figure 4. Yarn Tenacity and Elongation as a Function of the Actual Draw Ratio

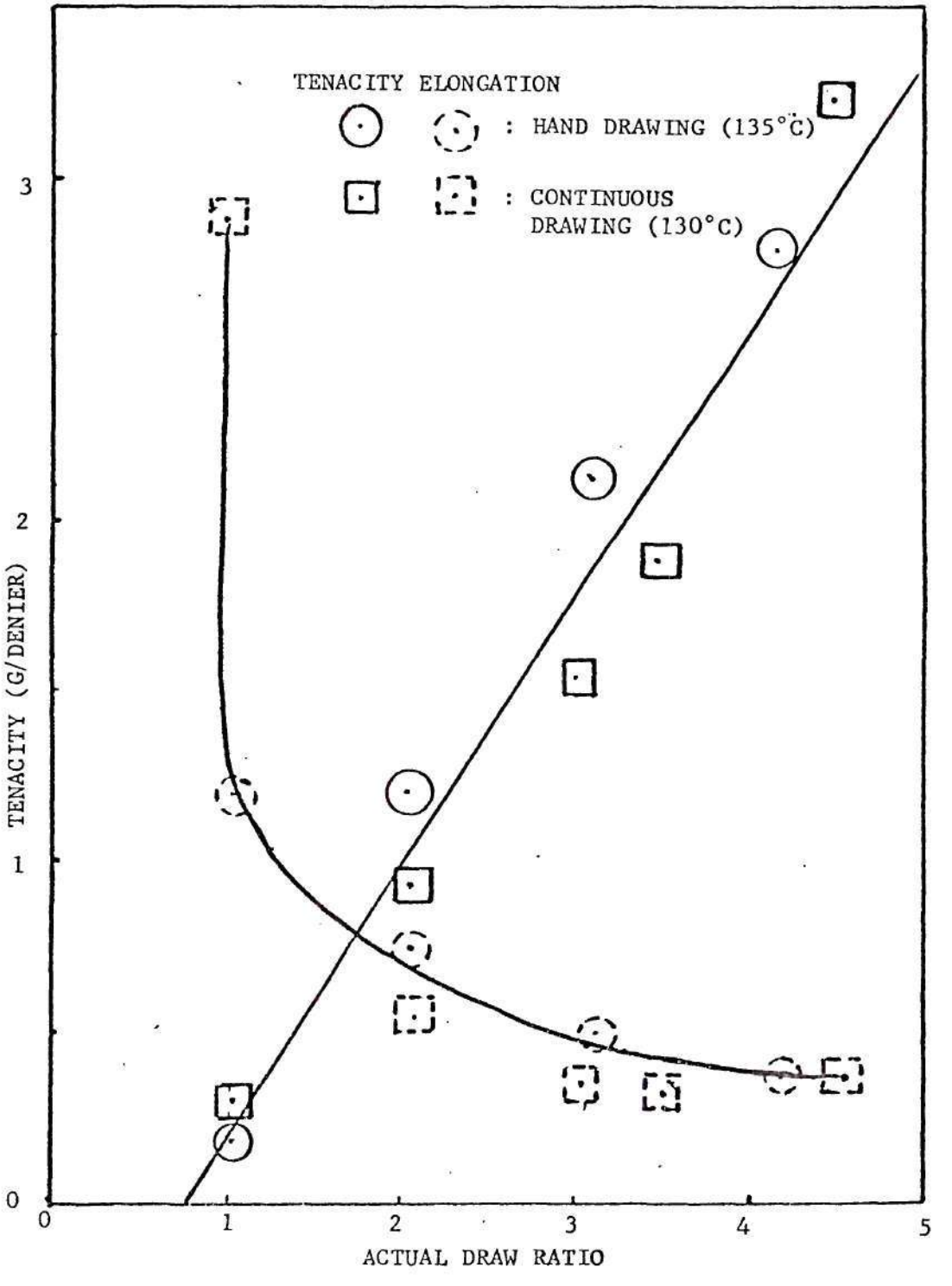

Figure 5. Comparison of Hand and Continuous Drawn Yarns

The actual draw ratios obtained were achieved by sequential and one step drawing. The actual draw ratio was changed in one step drawing by changing the relative speeds of the take-up and feed rollers (stretch ratio). The change in stretch ratio also changes the rate of deformation of the yarn in the drawing unit. However, Figure 4 suggests that no effect is derived from different elongation rates because there is no divergence from the straight line behavior of tenacity and actual draw ratio.

The actual draw ratio measured from the denier was lower than the nominal draw ratio imposed by the stretch ratio of each run through the oven. The difference in the draw ratios was quantified as the nominal draw ratio minus the actual draw ratio (NDR-ADR=ΔDR). The effects of the nominal draw ratio for one run (stretch ratio), temperature, and feed velocity on ΔDR are shown in Figures 6, 7, and 8, respectively. A higher nominal draw ratio and a lower temperature induce more variance in the measured and imposed draw ratios. Feed velocity did not change the variance significantly for speeds of 8.2 to 135 FPM, but the tendency was for an increase in ΔDR at lower speeds.

These trends point to slippage at the rollers as the major reason for less actual draw. At higher nominal draw ratios, a higher tension is applied to achieve an increased elongation during the length of the box; therefore, a higher tension is transmitted to the feed rollers increasing the driving force for slippage at both rollers. Likewise, an increased rate of elongation modifies the stress-strain relation in the same way as a decrease in temperature; the stress necessary to produce a specific elongation increases with decreasing temperature. Both an

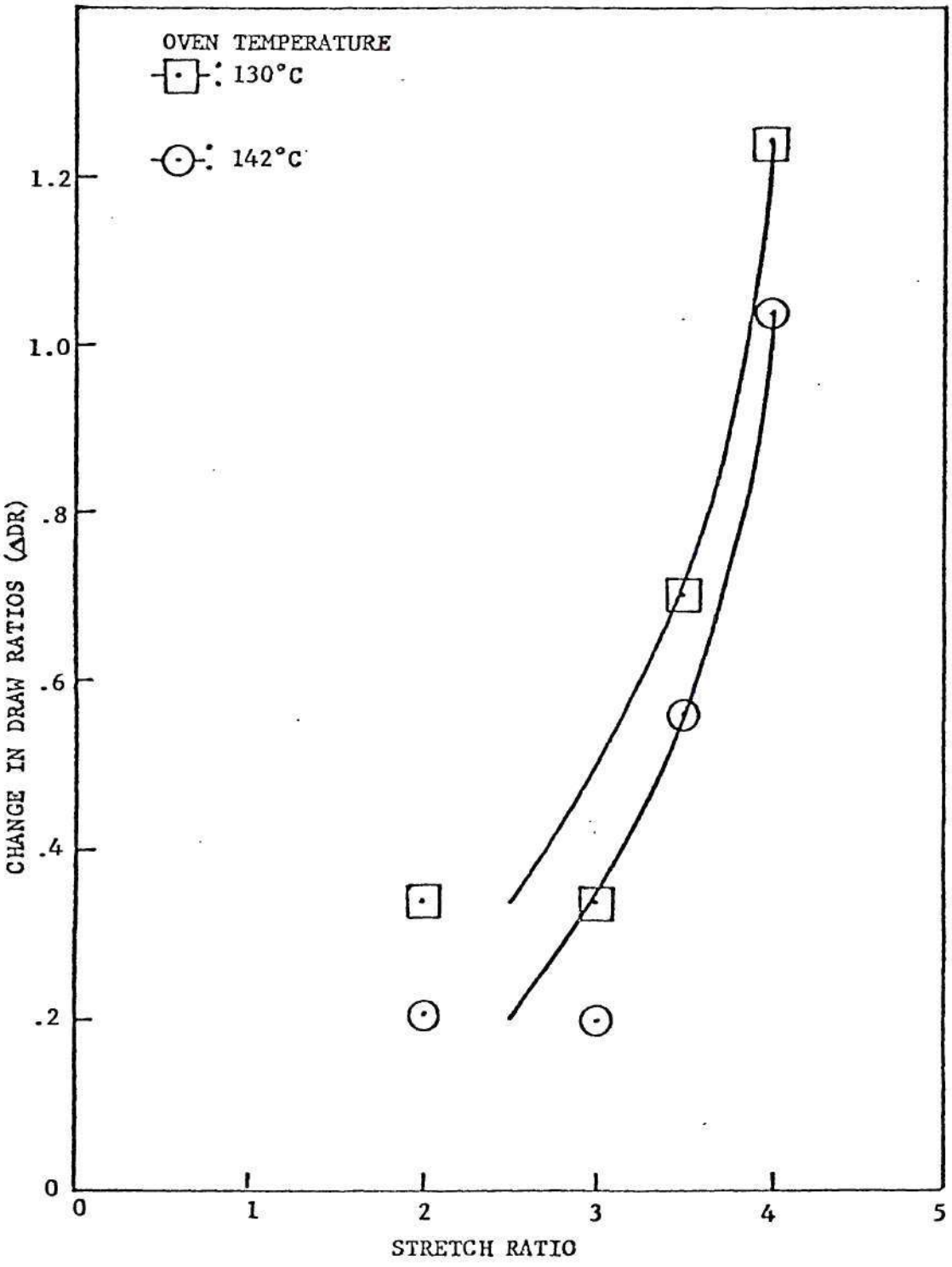

Figure 6. The Change in Draw Ratios (ΔDR) as a Function of the Stretch Ratio Plotted at 130°C and 142°C

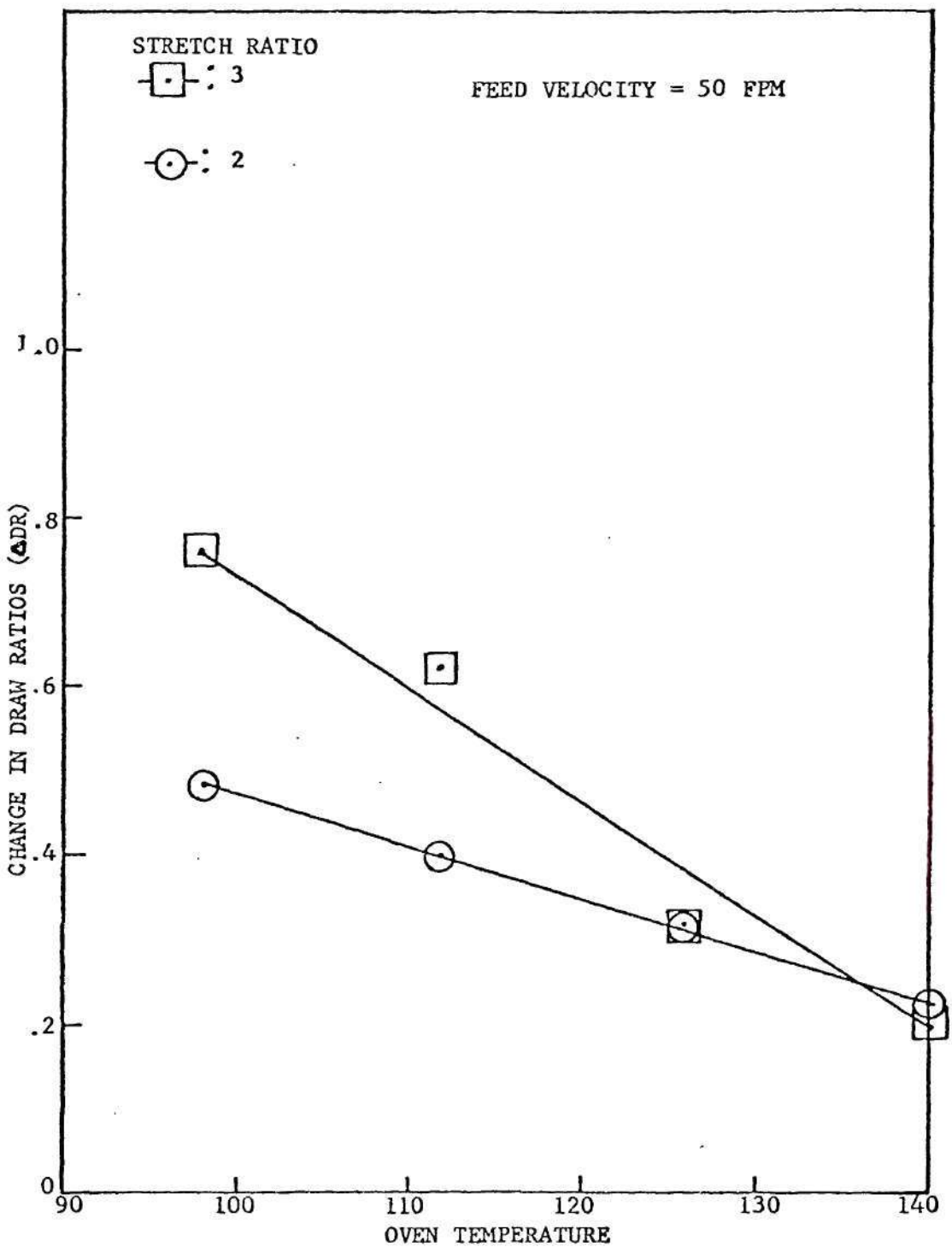

Figure 7. The Change in Draw Ratios (ΔDR) as a Function of the Oven Temperature Plotted Using a Stretch Ratio of 2 and 3

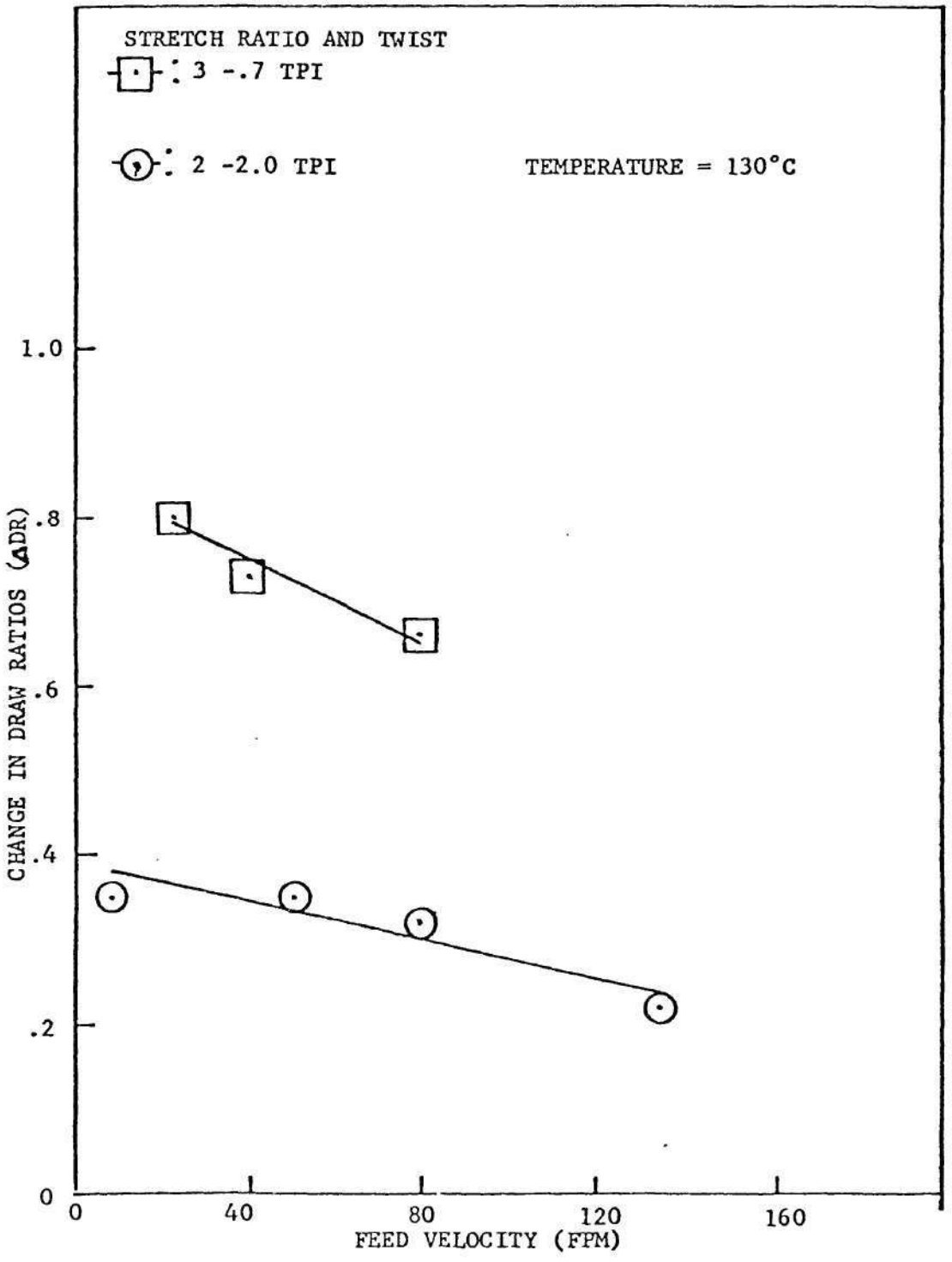

Figure 8. The Change in Draw Ratios (ΔDR) as a Function of the Feed Velocity Plotted Using a Stretch Ratio of 2 and 3

increase in the rate of elongation and a decrease in temperature cause the tension necessary for elongation to go up, therefore, the driving force for slippage is increased. Higher feed velocities decrease slippage because the residence time between the rollers is lower so there is less time to slip, but this effect is slight. Additional mechanisms which might affect the variance in draw ratios (actual and imposed), are elastic recovery and relaxation effects. These effects have been shown to play a minor role in the temperature range of this study [15].

4.3 Feed Velocity and Temperature

The tenacity is observed in Figure 9 as a function of draw ratio at feed velocities of 10, 50, and 100 FPM. The similarity between this plot and Figure 4 with constant feed velocity confirms that the rate of elongation due to a variable feed velocity does not influence the tenacity of the sample yarns within the scope of the measurements.

Plotting draw ratio versus tenacity and elongation using oven temperatures of 95 to 142°C produces a plot consistent with using a constant temperature as in Figure 4 (see Figure 10). Therefore, the influence of drawing temperature on tenacity and elongation is smaller than the experimental error involved in this study for this temperature range.

4.4 Twist

In contrast, twist shows a noticeable effect on the tenacity and elongation as shown in Figure 11. The maximum tenacity reached with increasing twist occurs at 5 TPI. The elongation increases with increasing twist. Park suggested about his similar findings that twist introduces mutual cohesion between the filaments. Another reason for an increase in

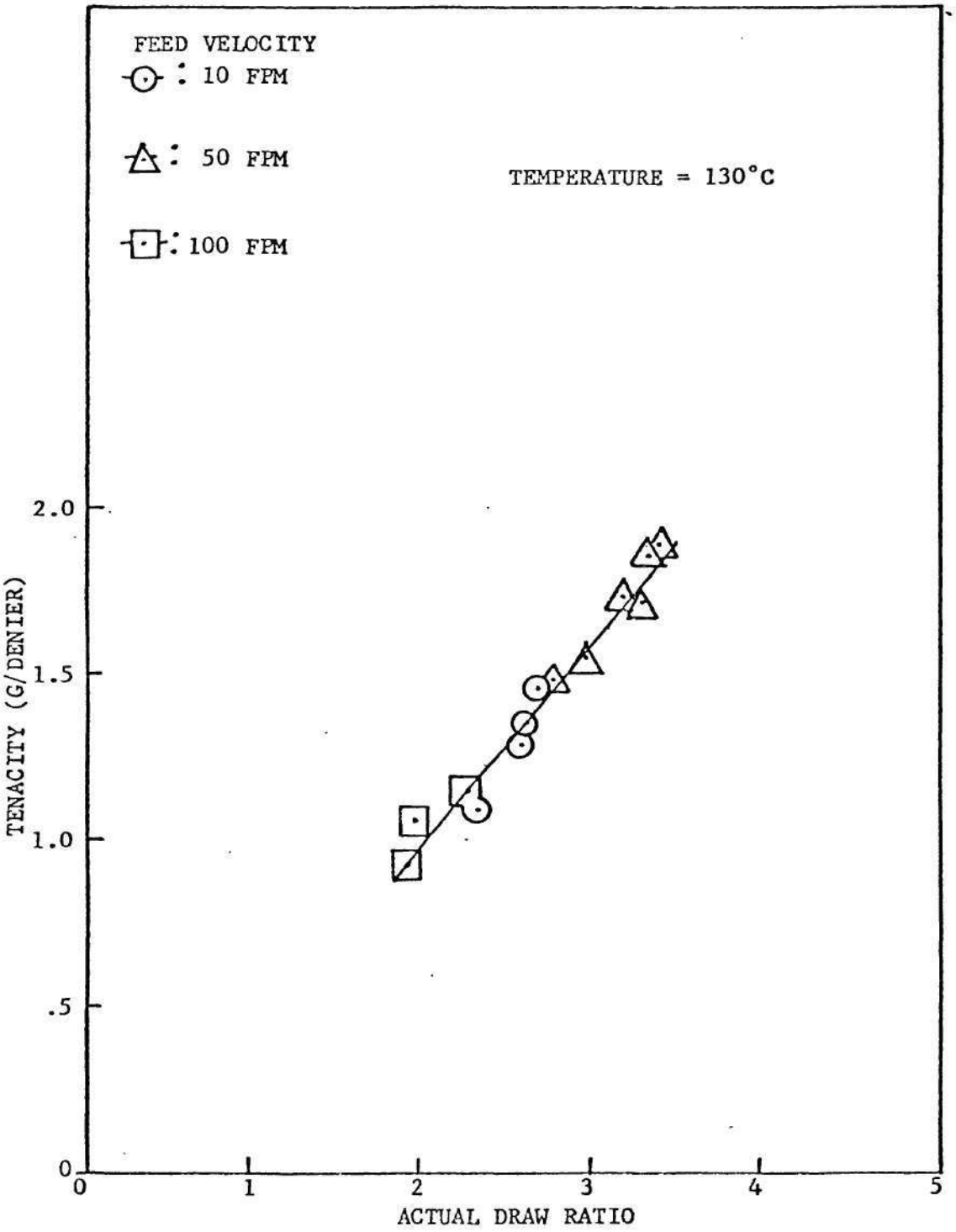

Figure 9. Yarn Tenacity as a Function of Draw Ratio Using Feed Velocities of 10, 50, and 100 FPM

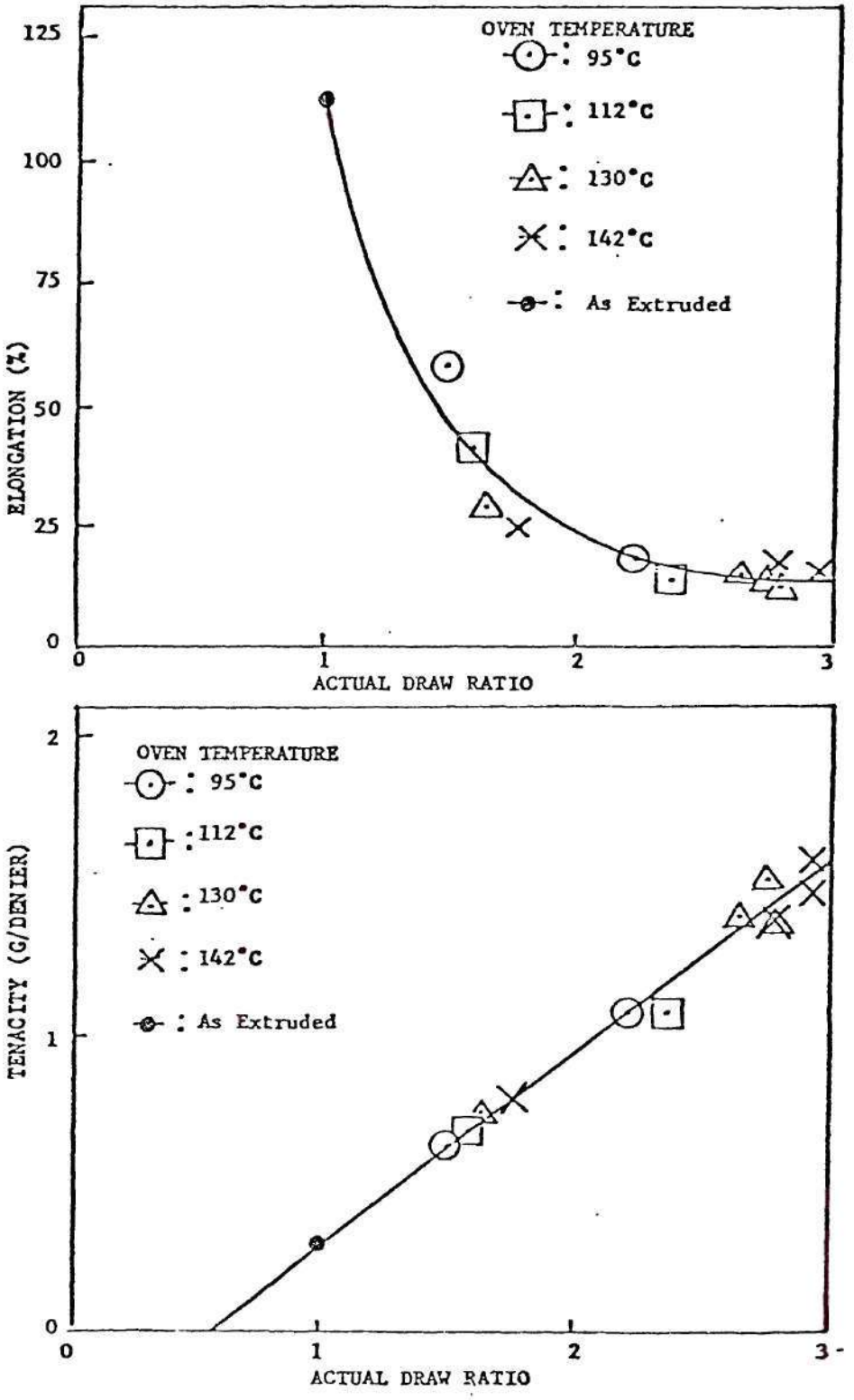

Figure 10. Yarn Tenacity and Elongation as a Function of Draw Ratio Using Temperatures of 95, 112, 130 and 142°C

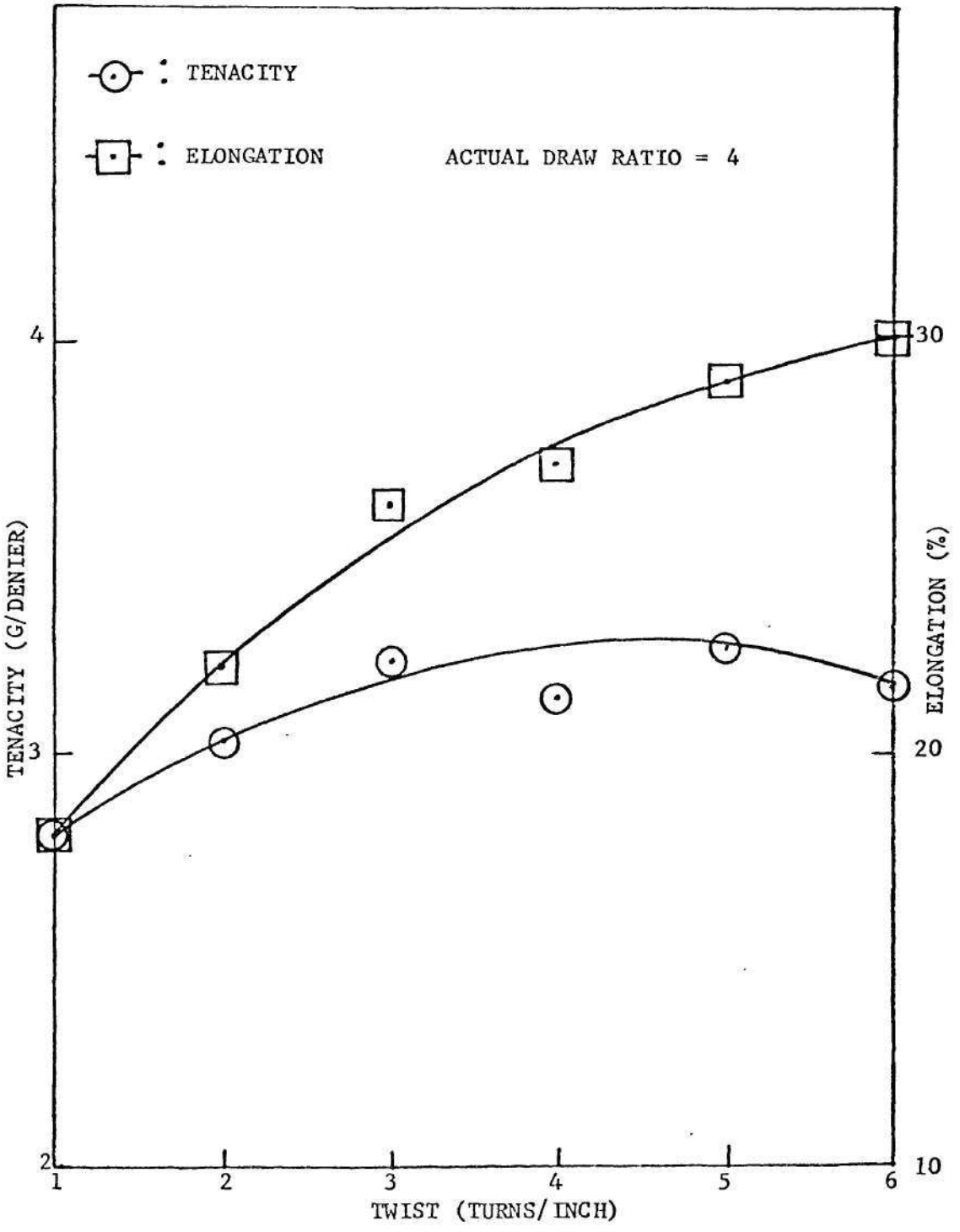

Figure 11. Yarn Tenacity and Elongation as a Function of Twist

tenacity of more importance is fiber migration. In order for the filaments to conform to the helical path, the longer filaments tend to move to the outside while the shorter filaments move to the shorter inside path. This migration tends to allow a more uniform distribution of the stress among the filaments. The bulkier, less elongated filaments would migrate to the center where the drawing process might preferentially draw them, thus explaining the improved drawing with twist. The migration would also be responsible for the increased tenacity since the load would be more uniformly distributed. The decrease in tenacity with twist above the maximum is attributed to filament obliquity [25].

4.5 Tenacity and Elongation

The tenacity and elongation are seen to be dependent primarily on the actual draw ratio and the twist applied to the foam fibrillated network yarn. The rate of elongation from either the draw ratio or the feed velocity has no observable effect on the yarn tenacity, nor does temperature produce any structural variations that affect the tenacity or elongation at break. Temperature and imposed draw ratio have a large influence on the slippage at the rollers of the drawing system; hence, these conditions must be considered when optimizing the drawing system.

4.6 Orientation

A higher actual draw ratio produces a higher tenacity, but no information as to the structural change of the yarn can be obtained from these measurements. Drawing of the foam fibrillated yarn is intended to stretch the individual filaments and therefore, cause molecular orientation and increased tenacity as it does in continuous filament drawing.

The possibility that the network yarn could thin out the superstructure rather than orienting the molecules is kept in mind while observing the effects that drawing has on the molecular structure.

Figure 12 shows the crystalline orientation (Hermans' Orientation Function) and the total molecular orientation (birefringence) as a function of the actual draw ratio. These relations follow the same trends observed in drawing of continuous filaments [26]. Figure 13 indicates the relationship between the crystalline orientation and the tenacity of the yarn. This agrees with the theories that an increase in orientation in the axial direction improves the strength of the polymer in that direction [24,26].

The birefringence (Δ_t) and crystalline orientation are compared in Figure 14 to show that the two measurements are consistent with the accepted literature relations [24]. The birefringence measurements are proportionately higher than Samuels [24] who uses a quartz compensator method rather than oils. There are two reasons for this discrepency. Using oils requires that the index of refraction be measured on two different filaments for the transverse and axial directions. The method revealed that there was considerable variance in the index of refraction in the axial direction, with the smaller size filaments having a higher molecular orientation. It was also revealed that each filament was made up of a bundle of smaller filaments having higher molecular orientation at the outer perimeter of the bundle. These structural phenomena made determination of an index of refraction a measurement of the average of several subjective readings, the method used would not allow the use of filaments that were lumpy or thick; therefore, preferential filament

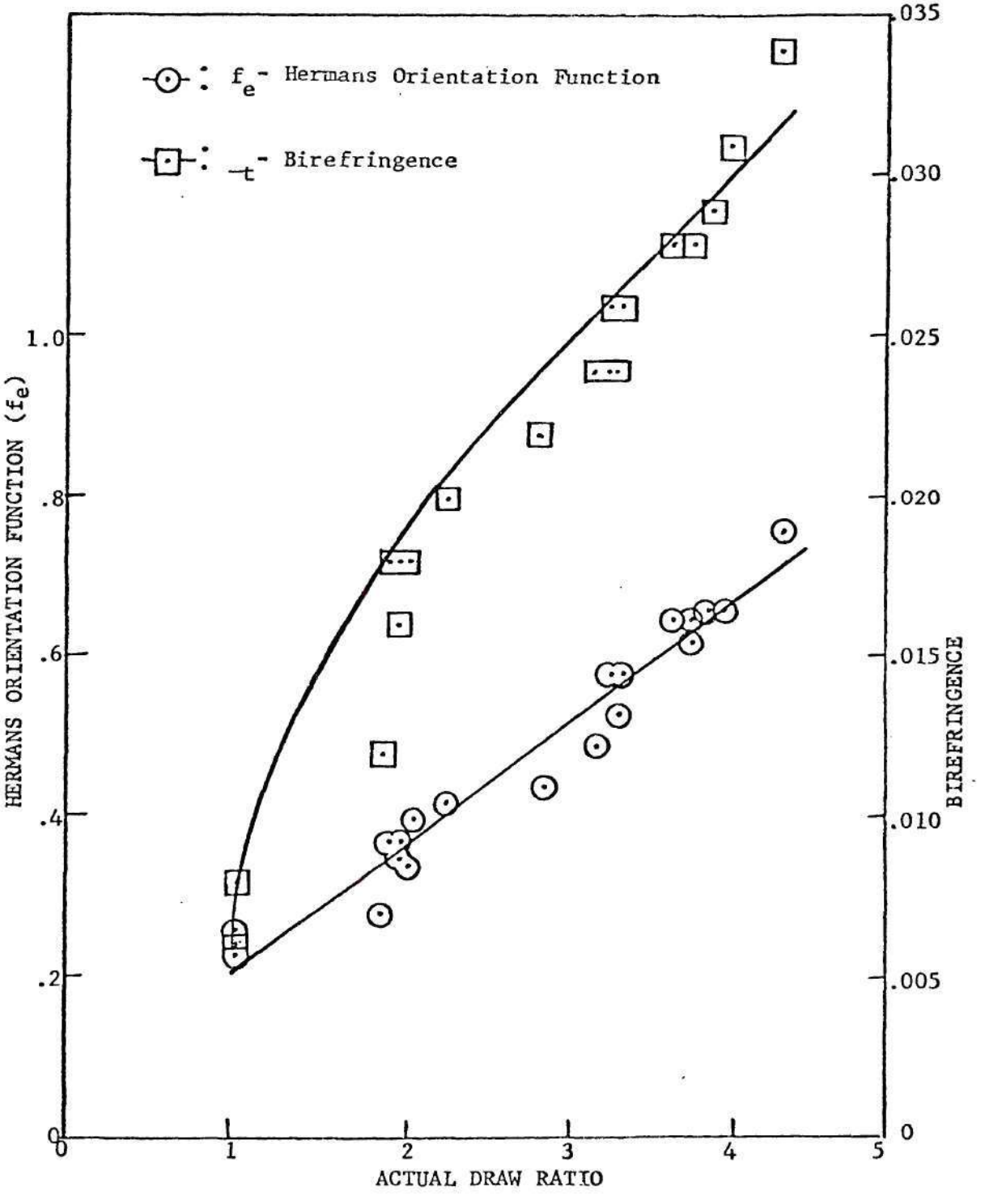

Figure 12. The Hermans' Orientation Function and Birefringence as a Function of the Actual Draw Ratio

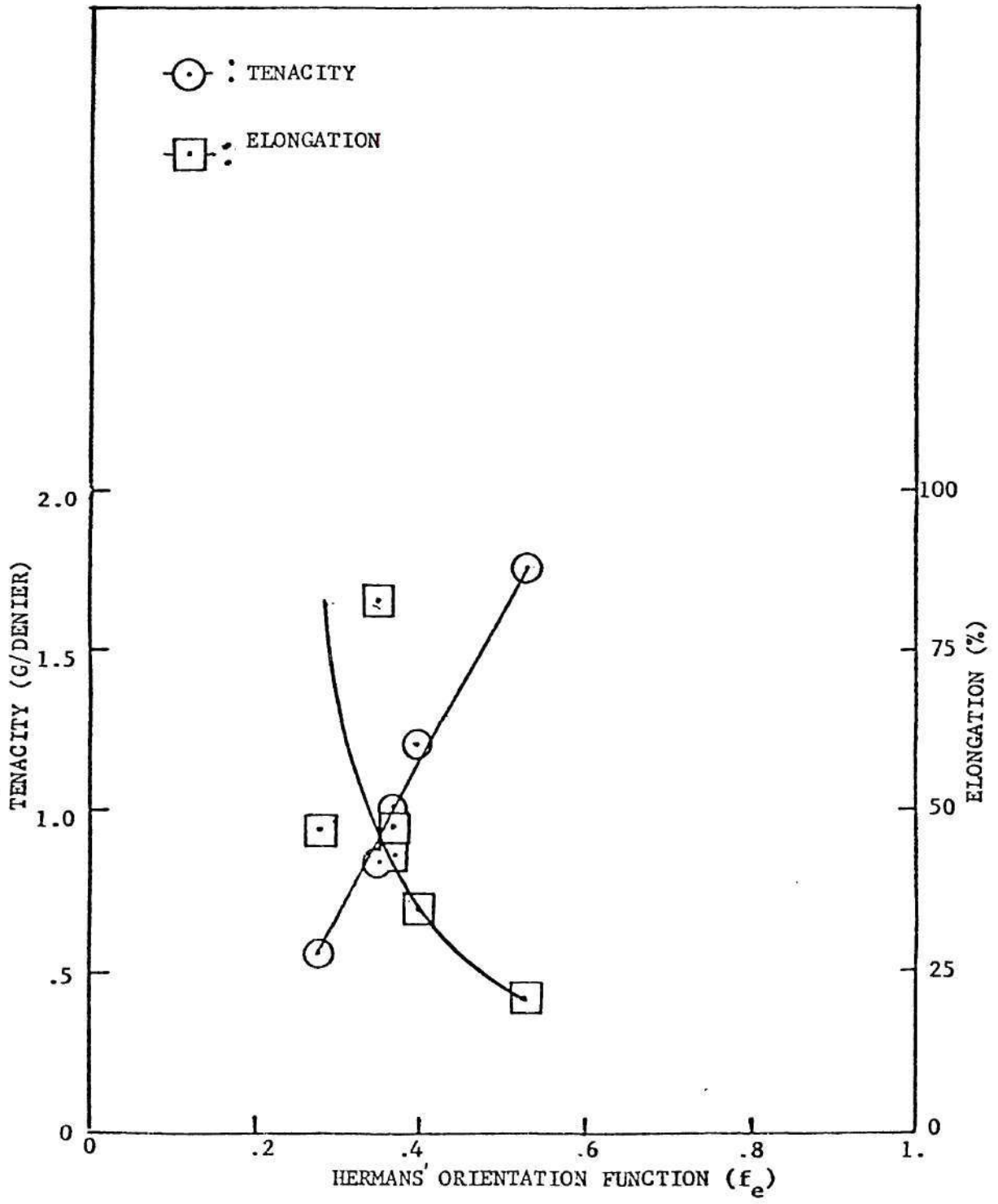

Figure 13. Yarn Tenacity and Elongation as a Function of the Hermans' Orientation Function (f_e)

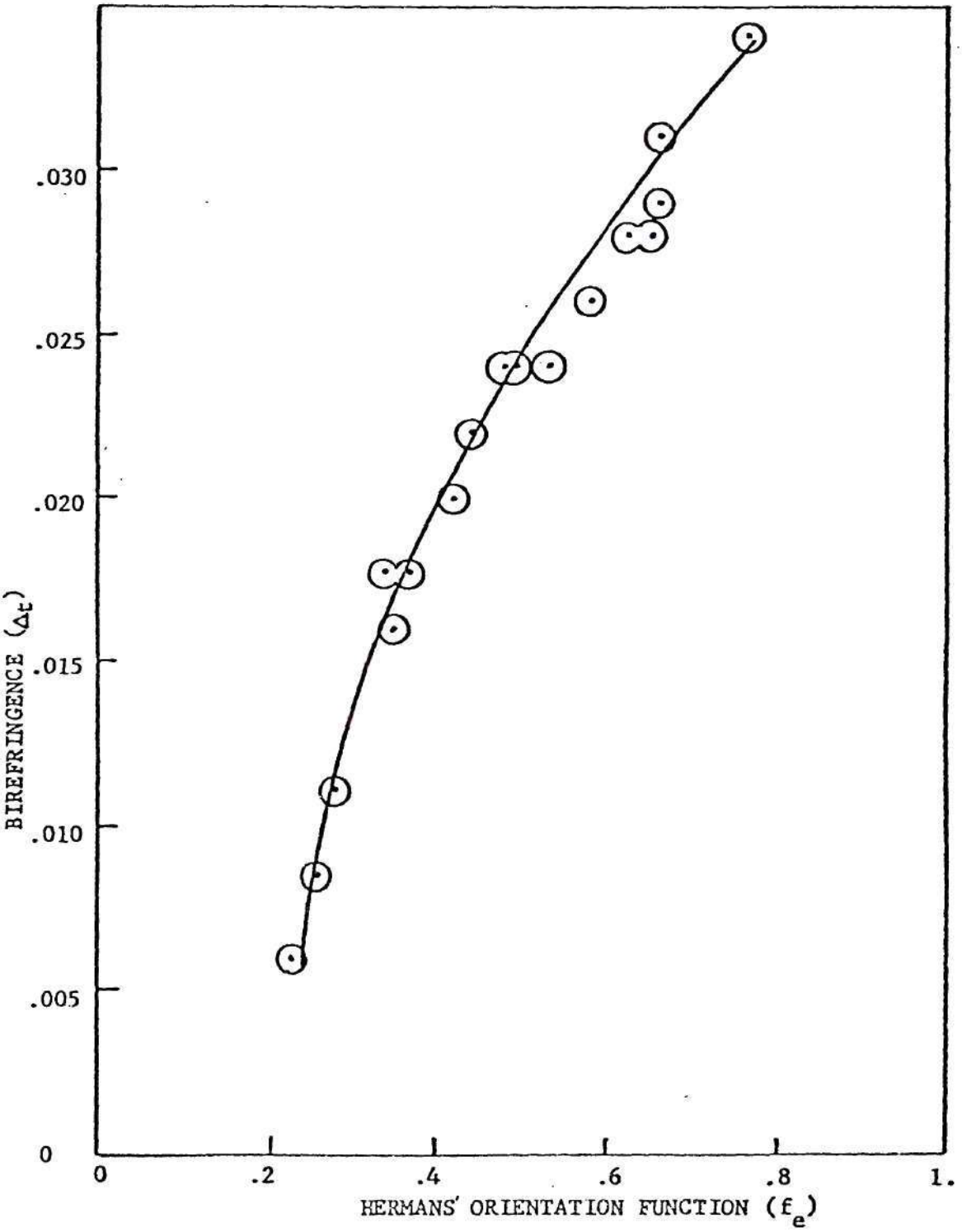

Figure 14. Birefringence as a Function of the Hermans' Orientation Function (f_e)

selection biases the results to the high side.

The amorphous and the crystalline phases contribute to the birefringence of the filament. Both phases increase in birefringence as the molecular orientation increases but the amorphous phase has a much higher contribution per unit mass. In order for the birefringence reading to reflect the molecular orientation, the relative amounts of crystalline and amorphous phases must not change [24]. The crystallinity was measured by X-ray diffraction to verify the birefringence measurements. The crystalline fraction was constant at 44% ±1% independent of draw ratio, therefore the birefringence reflects the molecular orientation change. Using the birefringence, the crystallinity, and the crystalline orientation (f_e), it was attempted to calculate the amorphous orientation from a relation suggested by Samuels [24]. The technique did not give realistic amorphous orientations because the birefringence was a measurement including only the finer, more oriented filaments while the other two measurements were done by X-ray diffraction which included the lumpy, less oriented filaments in the determination.

A comparison of the network yarn's tenacity versus orientation of the crystalline phase is made with monofilaments in Figure 15. The monofilaments were drawn in conventional textile drawing machinery by Sheehan, Wellman, and Cole [26]. The difference in crystalline orientation at the same tenacity points out the variance in techniques employed for X-ray analysis (see Appendix A). The general trend for an increase in tenacity with higher orientation holds true for both monofilaments and the network yarns.

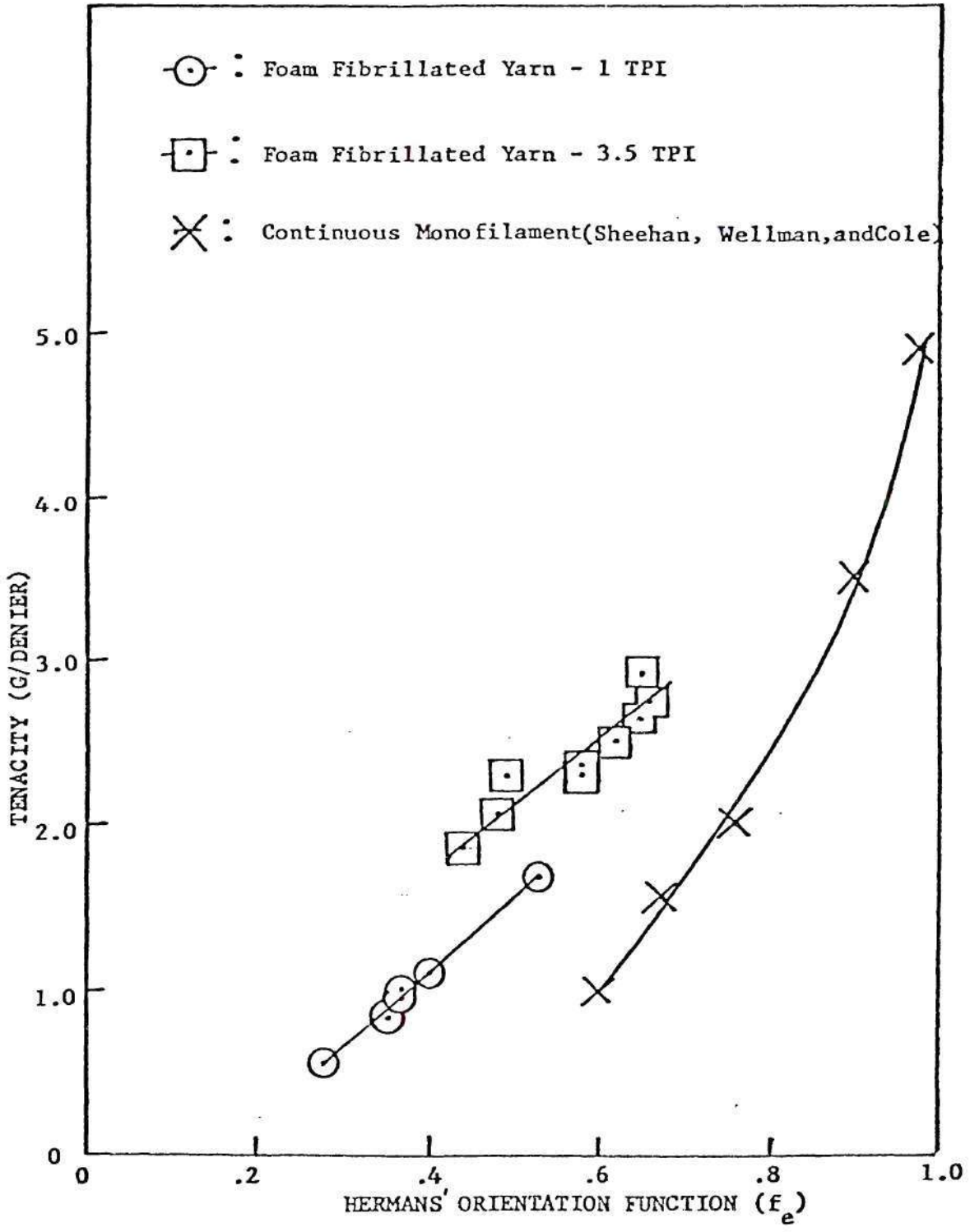

Figure 15. Comparison of Yarn Tenacity of Foam Fibrillated Yarn and Monofilament as a Function of the Hermans' Orientation Function

4.7 Size Analysis

The investigation of the cross sections revealed that the filaments have a ribbon shaped geometry (see Figure 16). It was found that the number of filaments per cross section increases with increasing draw ratio. The number of filaments in one yarn sample increased from 122 for the undrawn yarn to 256 and 287 after drawing the yarn two times and four times, respectively.

The size distribution illustrates the number of filaments with a specific dimension for both the width and the thickness of the filament ribbon. Figures 17, 18, and 19 show the size distribution for yarn samples with undrawn conditions, a draw ratio of two, and a draw ratio of four, respectively. In these figures, the length of the lines indicate the relative number of filaments with the specified size (1 mm = 1 filament). The change in size distribution is noticeable as the ribbons become smaller and the distribution becomes sharper.

Figure 20 contrasts the undrawn yarn to a yarn with a draw ratio of two. The axial view points out the increase in fine texture accomplished by drawing.

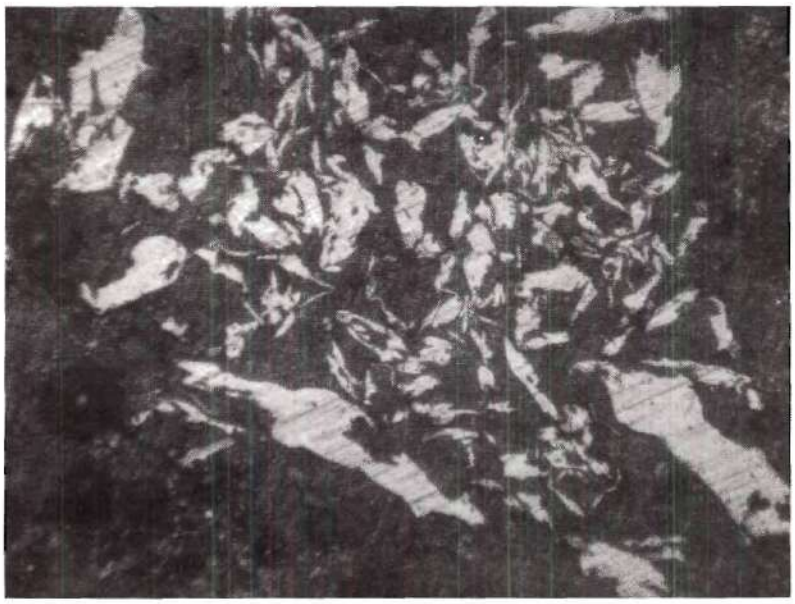

Figure 16. Foam Fibrillated Yarn Cross Section with Actual Draw Ratio of 2

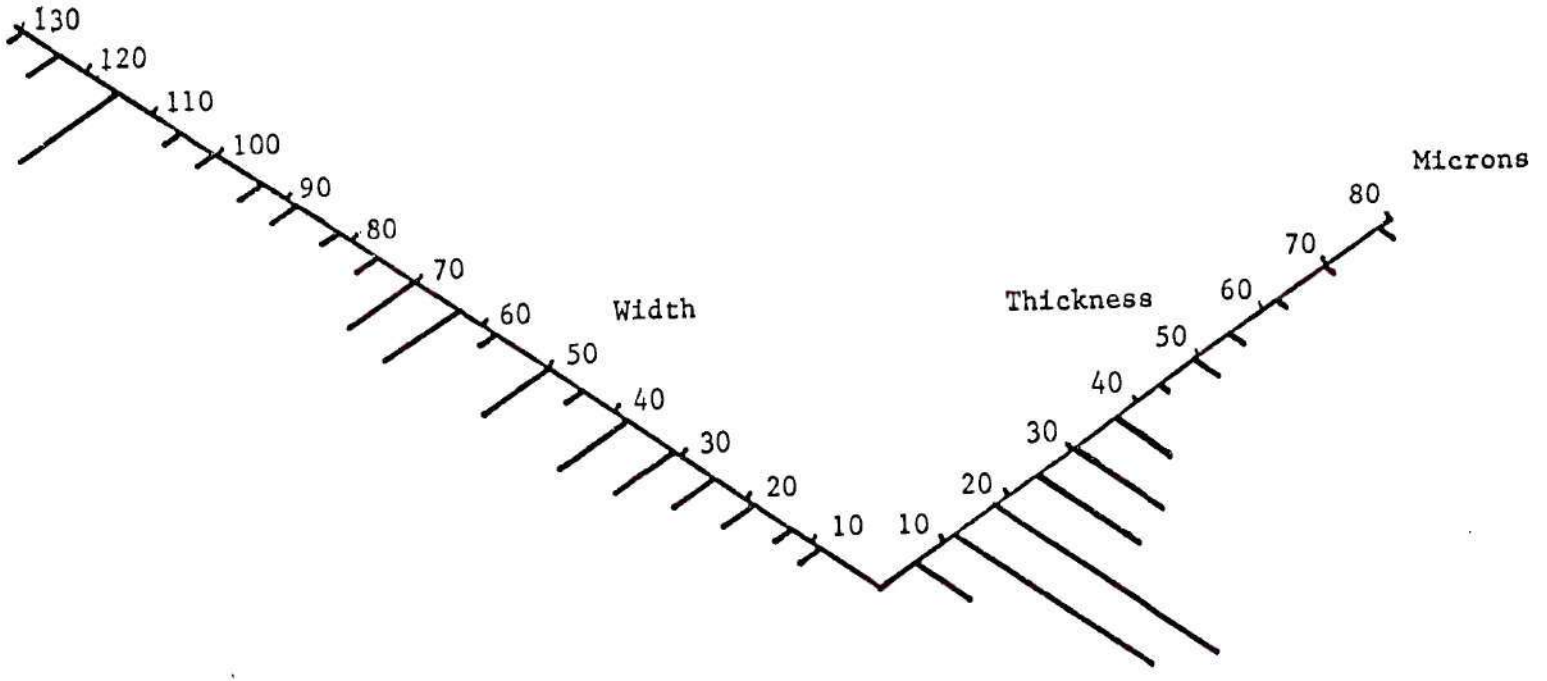

Figure 17. Filament Size Distribution of an Undrawn Yarn

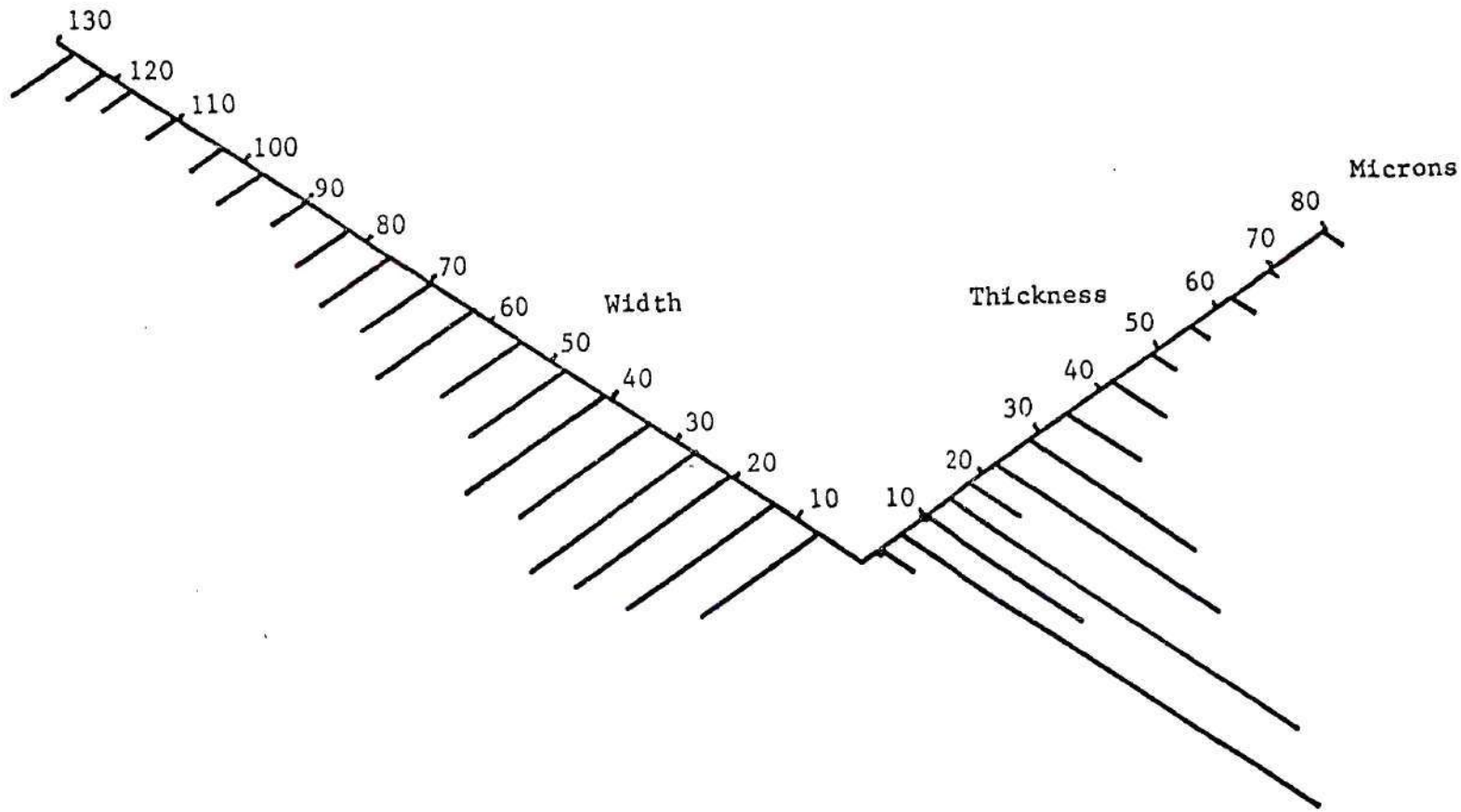

Figure 18. Filament Size Distribution of a Yarn With Actual Draw Ratio of 2

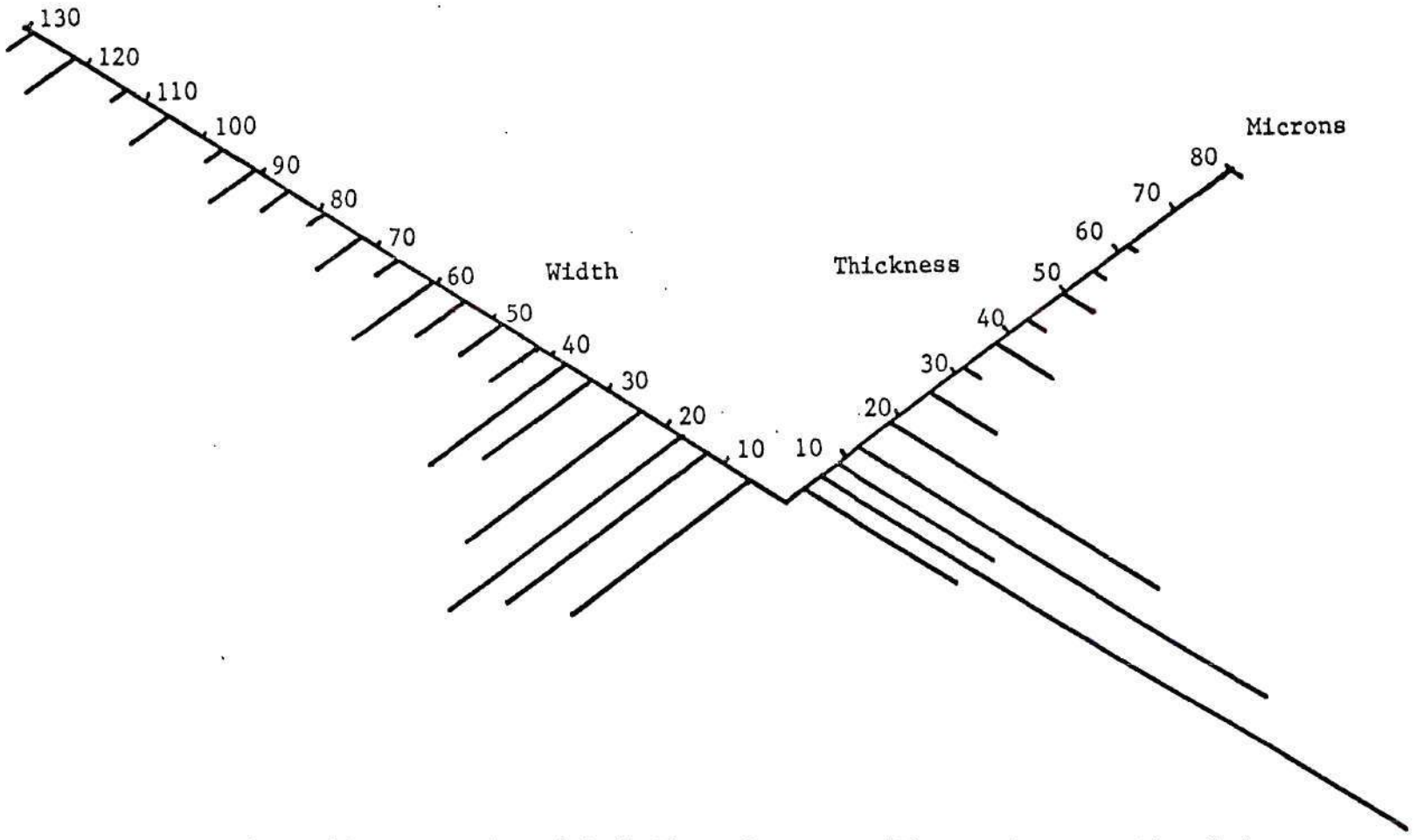

Figure 19. Yarn Size Distribution of a Yarn with Actual Draw Ratio of 4

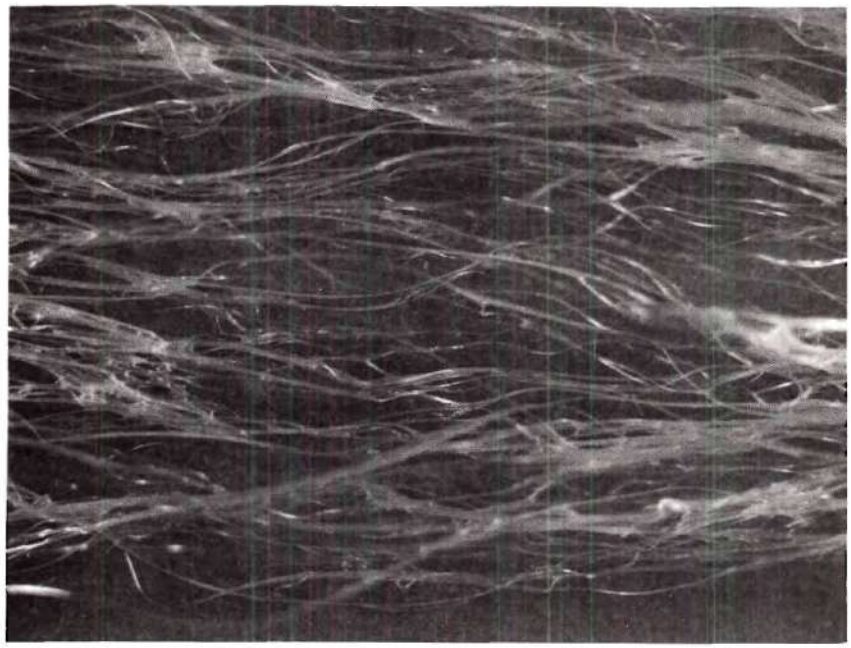

(a)

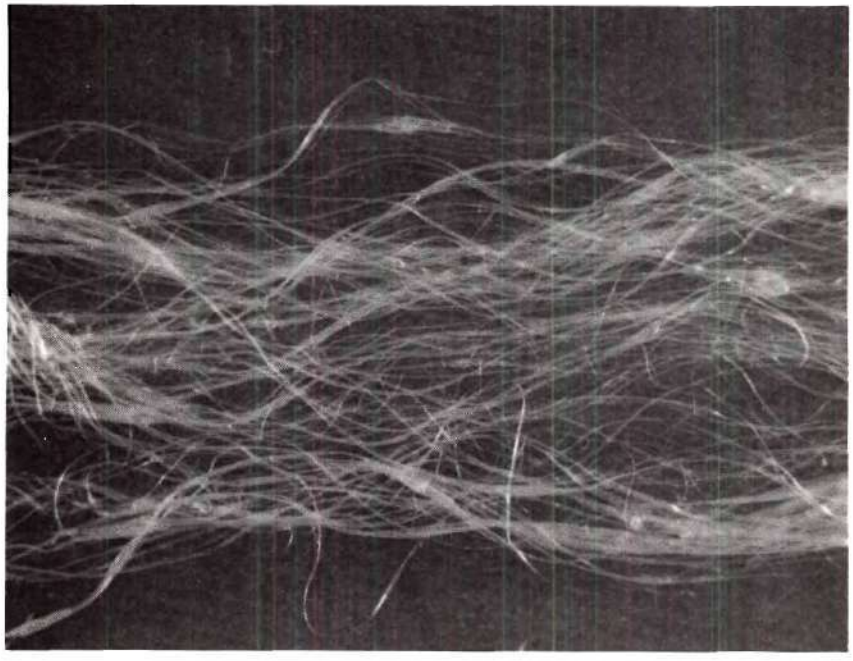

(b)

Figure 20. Longitudinal View of Yarns
a) Undrawn Yarn
b) Drawn Yarn(Actual Draw Ratio of 2)

CHAPTER V

CONCLUSIONS AND RECOMMENDATIONS

5.1 Conclusions

Continuous drawing of a biaxially stretched foam fibrillated yarn can produce yarns with tenacities of commercial value (greater than 2 g/denier). Drawing causes the tenacity to increase while the elongation asymptotically approaches 15 to 25% at break for a draw ratio of four. Twist is needed to provide the parent (undrawn) yarn with enough strength to successfully draw it in the continuous drawing system.

Investigation of the variables involved in drawing shows that the actual draw ratio obtained is most important in determining the tenacity of the yarn. Twist produces an optimum tenacity at 5 TPI for a yarn drawn four times. The temperature and rate of elongation of the yarn in the drawing oven do not have an effect on the tenacity or elongation at break over the range studied; however, they are important in optimizing the draw ratio achieved since they affect the slippage at the rollers.

Structural study indicates a constant increase in molecular orientation as the actual draw ratio increases. The ribbon shaped filaments decrease in size with increasing draw ratio as indicated by the cross-sectional size distribution. Since the number of filaments increases with draw ratio, apparently the superstructure continues to fibrillate into finer members in conjunction with the elongation of filaments during drawing. These phenomena result in higher axial strength and

increased flexibility. Breakage of filaments was not significant in this study.

5.2 Recommendations

The uniformity of the web is crucial as a variable in the process but its evaluation is contingent on the drawn yarn produced; therefore, a comprehensive look at the extrusion and drawing of the yarn with an emphasis on the final product is recommended.

The overall aim of a continuous line process, from foam extrusion to drawn yarn, might be accomplished if false twisting were introduced prior to drawing. False twisting should provide the twist needed for continuous drawing while circumventing the necessity of a discontinuous twisting operation. The unique qualities of the foam fibrillated yarn might also be enhanced by the extra bulk introduced by false twist texturing.

The use of other fiber forming polymers would allow the foam fibrillation process more acceptance as an economically feasible concept and further research along these lines is in order.

Equipment Adjustments

The existing drawing system allowed a gap between the feed rollers and the drawing oven entrance (see Figure 2) where the pop of filaments breaking could be heard. An improvement would be to construct a drawing oven which was flush with the rollers as in conventional drawing machinery.

Testing Procedures

The cross-sectional preparation of the sample yarns should be attempted using accepted textile methods of microtoming in an appropriate

medium. An ionizing vapor deposition (sputtering) of the gold-palladium alloy used in electron microscopy to coat the fiber samples might allow a better contrast between the medium and the filament cross section while defining the perimeter of the filaments.

APPENDIX A

THE DETERMINATION OF THE CRYSTALLINE ORIENTATION

A.1 Introduction

Drawing polypropylene fiber results in an orientation of both crystalline and amorphous regions to the axial direction, hence an increased axial strength. The change in the orientation of the crystalline region of the fiber can be determined in the same fashion that metal textures are measured. X-ray diffraction intensities of one diffracting plane are measured in all possible directions and the intensities are compared to decide which direction has the greatest number of diffracting planes. Fortunately, fiber orientation is limited to the transverse and the axial directions, therefore a two-dimensional investigation of the yarn structure gives a complete picture. This study uses polypropylene's strongest diffraction peaks, the (110) and the (040) unit cell planes, to determine the orientation of the c-axis of the unit cell. The c-axis is parallel to the helical axis of the molecule, therefore by determining the average angle the c-axis makes with the fiber axis, one has obtained a function of the average orientation of the molecules with respect to the axial direction.

Wilchinsky [23] derived an expression for the geometrical relationship between the two diffraction planes and the c-axis plane (001):

$$\cos^2\phi_{001} = 1 - \frac{\cos^2\phi_{110} - ((1-2\sin(72.5))\cos^2\phi_{040})}{\sin^2(72.5)}$$

where $\cos^2\phi_{hkl}$ is the average angle the (hkl) plane makes with the fiber axis.

The average angle the diffracting planes make with the axial direction are calculated from the intensity measurements, I(p), by the following equation.

$$\cos^2\phi_{hkl} = \cos^2\theta \times \frac{\int_0^{\pi/2} I(p) \cos^2 p \sin p \, dp}{\int_0^{\pi/2} I(p) \sin p \, dp}$$

where θ is the angle at which the (hkl) plane is inclined to the incident beam, and p is the azimuthal angle (the angle between the stretch direction and the plane of measurement of the diffraction intensity.

Hermans developed an orientation function for the c-axis from the orientation angle of the (001) plane of interest which varies from 1 to -.5 corresponding to an average angle of 0 to 90 degrees with the reference direction.

$$f_e = (3\cos^2\phi_{001} - 1)/2$$

A.2 Intensity Measurements

In order to measure the intensity of the diffraction peaks, the yarn had to be mounted in a plane perpendicular to the incident X-ray beam. Several strands of yarn were mounted parallel to each other so that the filament axes ran uniformly in one direction. The sheet of filaments formed was rotated about the axis of the beam 90 degrees,

retaining the sample plane perpendicular to the beam.

Unfortunately, the incident beam was rectangular in shape; therefore, the crystalline density exposed to the beam was subject to variation with the rotation angle. Preparation of the sample prior to diffraction did not insure a constant crystalline density, so the sample had to be mounted so that a diffraction test could determine the variance in the number of diffraction planes exposed to the beam with rotation. The method employed was made on the assumption that intensity diffracted above $2\theta = 40$ degrees is a function of the incoherent and diffuse scattering of the crystalline planes and the amorphous material exposed in the beam and is independent of orientation effects. A 2θ angle of 50 degrees was scanned along the azimuthal angle; if the intensity reading was constant with angle rotation, the procedure of scanning the two diffraction peaks was carried out. The samples were mounted again if the intensity readings varied. The intensity readings were gathered from a photomultiplier. The 90 degree azimuthal scan was observed in 5 degree increments and the diffraction intensities were corrected for incoherent and diffuse scattering, and background intensity prior to calculating f_e. Sheehan, Wellman and Cole studied crystalline orientation of polypropylene monofilaments using photodensity measurements, and pinhole collimation. This technique prevents crystalline density variation because the beam and the sample are not moved but the intensity readings are made by measuring the density of a photograph. However, these photographic intensity measurements are not accurate in comparison to photomultiplier readings.

APPENDIX B

THE DETERMINATION OF CRYSTALLINITY

Weidinger and Hermans [21] present a graphical procedure for determining the fraction of amorphous and crystalline phases in polypropylene. Both phases exhibit an X-ray diffraction peak; the amount of intensity each phase diffracts per unit mass is not theoretically well understood [22].

The intensities of each component occur at the same diffraction angles, so an empirical separation of the intensities is outlined. The effect of crystallinity on the relative intensities was calculated by linear regression, resulting in the following formula:

$$x = \frac{1}{1 + 1.297(I_{am}/I_{cr})}$$

where

x = crystalline fraction

I_{am} = integrated amorphous intensity contribution

I_{cr} = integrated crystalline intensity contribution

A diffracted pattern was taken over the Bragg angle from 10 to 30 degrees using a copper X-ray tube with a nickel filter which corresponds to a d-spacing range of 2.98 A to 8.85 A. The graphical procedure for dividing the intensity peak over the range into the amorphous and the crystalline contributions is outlined in the literature.

APPENDIX C

TABULATED DATA

ACTUAL DRAW RATIO	TENACITY G/DENIER	f_e	Δ_T $(I_{\|\|}-I_{\perp})$	$I_{\perp}$	$I_{\|\|}$	ACTUAL TPI	ΔDR	ELONGATION	DRYER TEMP.	CRY. (%)
1	.21	.23	.006	1.492	1.498	0		159		.42
1	.22	.28				0		174		
1	.27	.26	.008	1.494	1.502	0		168		.44
1.88	.56	.28	.012	1.486	1.498	1.06	.12	47	290	
1.92	.95	.37	.018	1.487	1.505	1.04	1.08	47	325	
1.96	.84	.35	.016	1.488	1.504	1.02	1.04	83	255	
1.98	1.00	.37	.018	1.488	1.506	1.01	1.02	43	255	
2.02	.92	.34	.018	1.487	1.505	.99	.98	82	220	
2.06	1.11	.40				.97	.94	34	255	
2.27	1.21	.42	.020	1.488	1.508	.88	.73	34	290	.45
2.84	1.85	.44	.022	1.490	1.512	3.89	1.16	25	220	
3.19	2.30	.49	.024	1.488	1.512	3.74	.80	28	220	
3.22	2.07	.48	.024	1.492	1.516	3.73	.78	22	255	
3.29	2.36	.58	.026	1.490	1.514	3.71	.71	25	255	
3.32	1.67	.53	.024	1.492	1.516	2.00	1.18	20	290	
3.35	2.31	.58	.026	1.490	1.516	3.69	.65	25	290	
3.65	2.93	.65	.028	1.492	1.520	3.59	.35	32	290	
3.77	2.50	.62	.028	1.490	1.518	3.56	.23	29	325	
3.77	2.63	.65	.028	1.490	1.518	3.56	.23	24	290	
3.89	2.75	.66	.029	1.490	1.519	3.53	.11	23	325	.45
3.98	3.15	.66	.031	1.492	1.523	2.25	.89	24	290	
4.31	3.5	.76	.034	1.492	1.526	2.40	1.15	23	290	

BIBLIOGRAPHY

1. P. R. Lord, Spinning in the 70's, Merrow Pub.: London (1970), pp. 11, pp. 68-83.

2. P. G. Anderson, Textile Institute and Industry, 12(1), 203(1974).

3. A. Tweedale, Textile Institute and Industry, 12(1), 76(1974).

4. W. H. Badrian and J. H. L. Choufoer, The Textile Manufacturer, 97(1), 263(1971).

5. G. O. Thomas, The Textile Manufacturer, 97(1), 239(1971).

6. A. Newton and J. E. Ford, Textile Progress, 5(3), 68(1973).

7. B. C. Goswami, J. G. Martindale, and F. L. Scardino, Textile Yarns Technology, Structure, and Applications, Wiley and Sons Pub.: New York (1977), pp. 5-51, pp. 363-385.

8. Henry G. Schirmer, SPE Tech Papers, 20(1), 382(1974).

9. Herbert Blades, U.S.P. 3,227,784 (January 4, 1966).

10. P. Volans and P. D. Changani, Textile Institute 53rd Annual Conference, Studies in Modern Yarn Production, Manchester, England (1968).

11. J. D. Muzzy, G. H. Hoyos, A. R. Enuga, and Y. H. Park, SPE 35th Annual Technical Conference, Montreal Canada, April 25-28 (1977).

12. Andrzej, Ziabicki, Fundamentals of Fiber Formation, Wiley and Sons Pub.: New York (1976), pp. 389-450.

13. L. L. Scheiner, Plastics Technology, 23(1), 53(1977).

14. W. H. J. Badrian, Modern Textiles, 55(1), 58(1974).

15. H. F. Mark, S. M. Atlas, and E. Cernia, Man-Made Fibers, Wiley and Sons Pub.: New York (1967), vol. 1, pp. 169-223.

16. H. F. Mark, S. M. Atlas, and E. Cernia, Man-Made Fibers, Wiley and Sons Pub.: New York (1967), vol. 3, pp. 185-190.

17. Y. H. Park, Yarn Formation By Blow-Film Extrusion, Master of Science Thesis, Georgia Institute of Technology, Atlanta, Georgia, (1977).

18. R. N. Hansen, SPE Journal, 18(1), 77(1962).

19. C. D. Han, Y. W. Kim, and K. D. Malhotra, Journal of Applied Polymer Science, 20(1), 1583(1976).

20. D. F. Bloss, An Introduction to the Methods of Optical Crystallography, Holt, Rinehart, and Winston: New York (1961), 67-73.

21. A. Weidinger and P. H. Hermans, Makromol. Chem., 50(1), 98(1961).

22. B. K. Vainshtein, Diffraction of X-rays by Chain Molecules, Elsevier Pub.: London (1966), p. 375.

23. Z. W. Wilchinsky, J. Applied Physics, 31(1), 1969(1960).

24. R. J. Samuels, Structured Polymer Properties, Wiley and Sons Pub.: New York (1974).

25. J. W. S. Hearle, P. Grosberg, and S. Backer, Structural Mechanics of Fibers, Yarns, and Fabrics, vol. 1, Wiley and Sons Pub.: New York (1969), p. 148.

26. W. C. Sheehan, R. E. Wellman, and T. B. Cole, Southern Research Institute Symposium on Polypropylene Fibers, September 17-18 (1964).

27. Roger Lacallade, Plastics Engineering, 32(1), 40(1976).